Computational Design and Performance Prediction of Creep-Resistant Ferritic Superalloys

(FE0024054)

Investigators: Peter K. Liaw[1], David C. Dunand[2], and Gautam Ghosh[2]

Collaborator: Chuan Zhang[3]

Students: Shao-Yu Wang[1], Zongyang Lyu[1], Gian Song[1], Zhiqian Sun[1], Michael Rawings[2], and Sungil Baik[2]

[1]The University of Tennessee, Knoxville (UTK)

[2]Northwestern University (NU)

[3]CompuTherm, LLC (CTL)

Northwestern

THE UNIVERSITY OF TENNESSEE KNOXVILLE

Acknowledgements

(1) Richard Dunst
(2) Vito Cedro
(3) Patricia Rawls
(4) Robert Romanosky
(5) Regis Conrad
(6) Jessica Mullen
(7) Mark D. Asta
(8) C. T. Liu
(9) Nicholas Anderson, for their kind support and encouragement, and
(11) National Energy Technology Laboratory (NETL) for sponsoring this project

Outline

- Technical Background of the Project
- Methods
- Current Progress
  - Modeling & Calculations
  - Experimental Results
- Papers, Presentations, and Awards
- Summaries and Current Status
- Future Plan

Technical Background of the Project

Each 1% increase in efficiency eliminates ~1,000,000 tons of CO_2 emissions over the lifetime of an 800-MW plant.

US-DOE Advanced Power System Goal 60% efficiency from coal generation Steam condition: 760 °C - 35 MPa

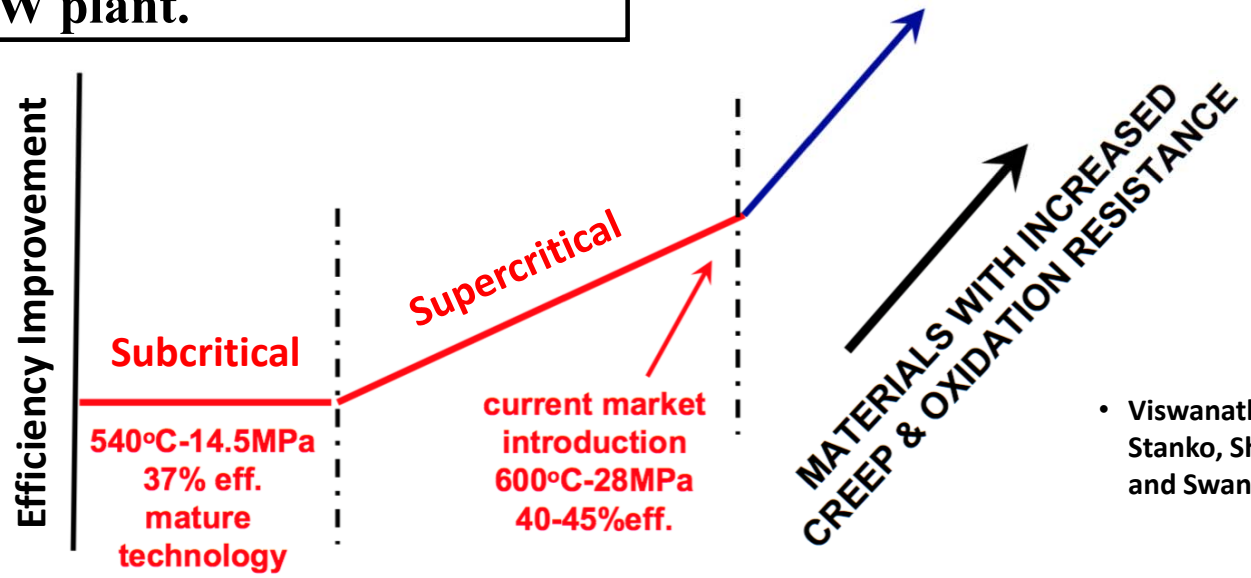

- Viswanathan, Henry, Tanzosh, Stanko, Shingledecker, Vitalis, Purgert, 2005, and Swanekamp, 2002

Plants operating above 22 MPa at 538 to 565 °C are "supercritical", and above 565 °C are "ultra-supercritical (USC)".

Technical Background of the Project (Cont'd)

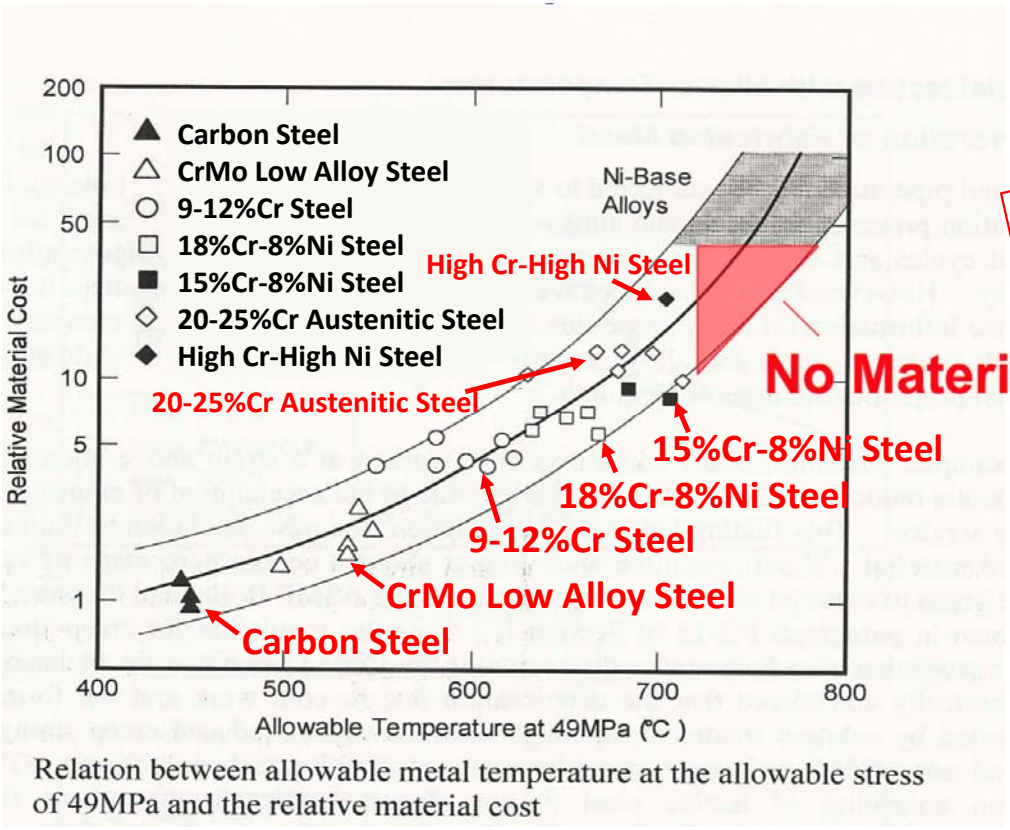

Relation between allowable metal temperature at the allowable stress of 49MPa and the relative material cost

https://www.netl.doe.gov/File%20Library/Events/2008/fem/Holcomb_pres.pdf

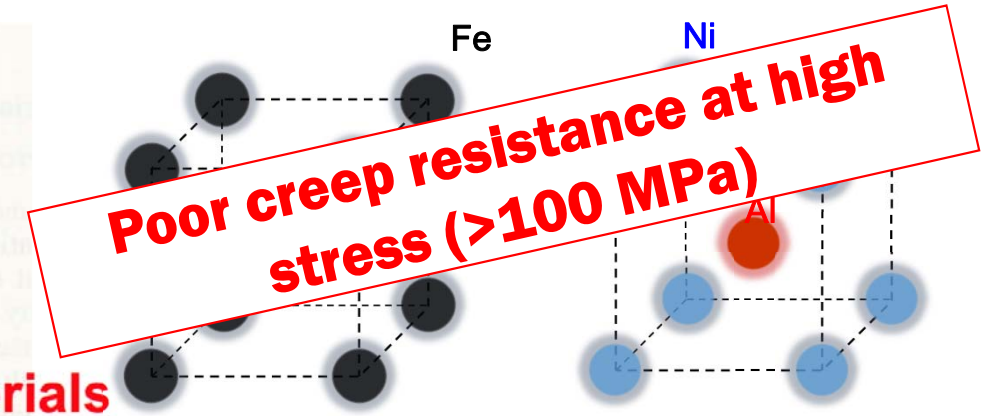

Fe (α phase) NiAl (B2 phase)

FBB8: Fe-6.5Al-10Cr-10Ni-3.4Mo-0.25Zr-0.005B, weight percent (wt.%)

By adding Ti, there will be $L2_1$-Ni_2TiAl formed. The creep strength of $L2_1$ between 753 and 1,000 °C is about three times that of NiAl.

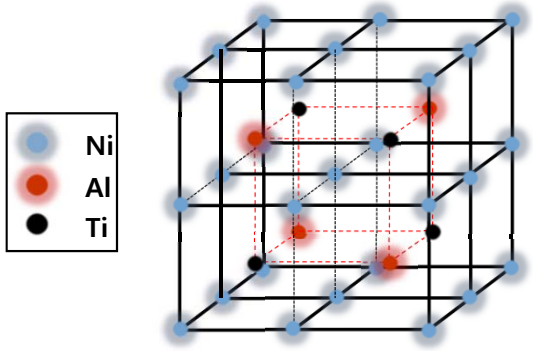

Ni_2TiAl ($L2_1$)

G. Song, Z. Sun, J. D. Poplawsky, Y. Gao, P. K. Liaw, Acta Mater., 127 (2017) 1-16.

G. Song, Z. Sun, L. Li, X. Xu, M. Rawlings, C.H. Liebscher, B. Clausen, J. Poplawsky, D.N. Leonard, S. Huang, Z. Teng, C.T. Liu, M.D. Asta, Y. Gao, D.C. Dunand, G. Ghosh, M. Chen, M.E. Fine, and P.K. Liaw, Scientific Report, 5 (2015) 16327.

Technical Background of the Project (Cont'd)

Objectives:

Based on FBB8 [Fe-6.5Al-10Cr-10Ni-3.4Mo-0.25Zr-0.025B (wt. %)]:

- **Develop and integrate modern computational tools and algorithms, i.e., predictive first-principles calculations, computational-thermodynamic modeling, and meso-scale dislocation dynamics simulations, to design high-temperature alloys for applications in fossil-energy-power plants.**

- **Understand the processing-microstructure-property-performance links underlying the creep behavior of novel ferritic alloys strengthened by hierarchical coherent B2/$L2_1$ precipitates.**

Technical Background of the Project (Cont'd)

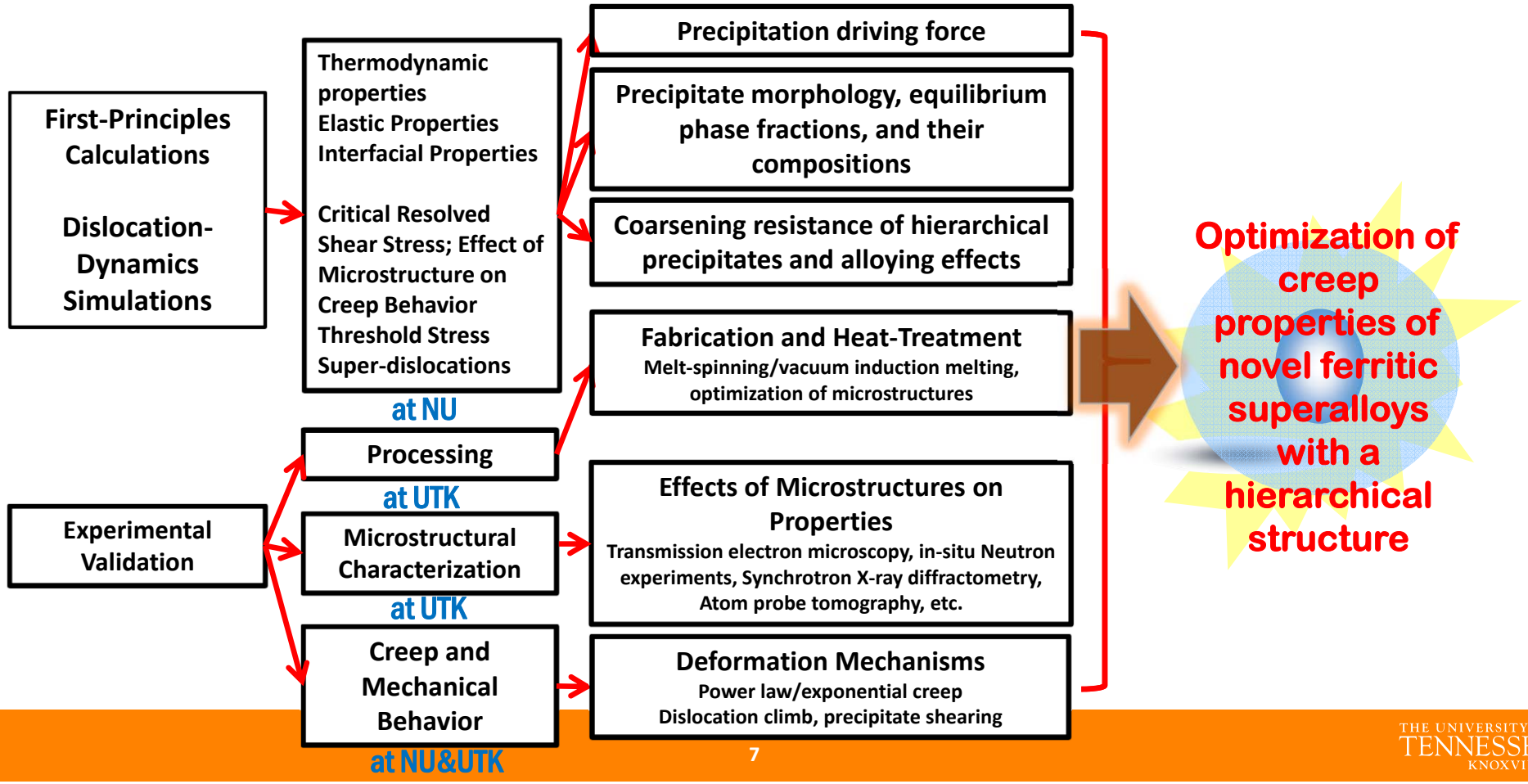

Methods - Computational - thermodynamic Modeling

- Conducting CALculation of PHAse Diagrams (CALPHAD)
- Requiring database, not available for every system.
- Providing information about phases, volume fractions…etc.

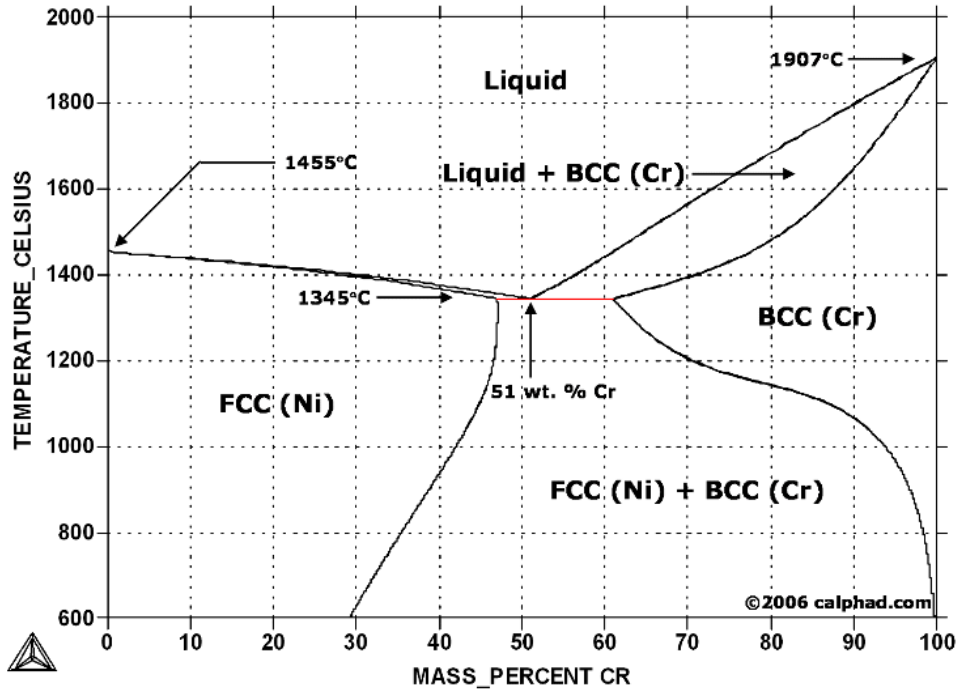

http://www.calphad.com/nickel-chromium.html

Methods - Predictive First-principles Calculations

- Calculation of single-crystal C_{ij}
- Two ab-initio approaches in this project: (1) energy density and (2) stress tensor

1) Energy density method uses total energy, *E*, as a function of deformation (e_i).

   - The *E*-e_i relationship allows us to extract C_{ij} values

2) Stress-tensor method (employs the generalized Hooke's law) to account for multi-axial loading and elastic anisotropy

Equilibrium Volume

Neglected

$$E(V,\{e_i\}) = E(v_0,0) - PV_0\sum_{i=1}^{3} e_i + \frac{V_0}{2}\sum_{i=1}^{6}\sum_{j=1}^{6} C_{ij}e_ie_j + O[e_i^3]$$

Total energy

Elastic energy under deformation

$$\begin{pmatrix}\sigma_1\\ \sigma_2\\ \sigma_3\\ \tau_1\\ \tau_2\\ \tau_3\end{pmatrix} = \begin{pmatrix} C_{11} & C_{12} & C_{12} & 0 & 0 & 0\\ C_{12} & C_{11} & C_{12} & 0 & 0 & 0\\ C_{12} & C_{12} & C_{11} & 0 & 0 & 0\\ 0 & 0 & 0 & C_{44} & 0 & 0\\ 0 & 0 & 0 & 0 & C_{44} & 0\\ 0 & 0 & 0 & 0 & 0 & C_{44}\end{pmatrix}\begin{pmatrix}\varepsilon_1\\ \varepsilon_2\\ \varepsilon_3\\ 2\gamma_1\\ 2\gamma_2\\ 2\gamma_3\end{pmatrix}$$

G. Ghosh and P. K. Liaw, in preparation, 2017

Methods - Experiments

- All alloy samples homogenized at 1,200 ^{o}C for 0.5 hour, and aged at 700 ^{o}C for 100 hours.

- Microstructural Characterization: scanning-electron microscopy (SEM), transmission-electron microscopy (TEM), local electrode atom-probe (LEAP), neutron/synchrotron diffraction techniques.

- Mechanical Tests: tensile and compressive creep tests.

Current Progress - Brief Summaries

Calculations

- First-principle Calculations on the elastic properties of α-Fe, B2-NiAl, and $L2_1$-Ni_2TiAl
- CALPHAD Calculations on FBB8 + Ti alloys and FBB8 + Zr alloys

FBB8 + Ti alloys

- In-situ Neutron
- TEM
- LEAP
- Creep Test

FBB8 + Hf alloys

- SEM
- TEM
- LEAP
- Creep Test

FBB8 + Zr alloys

- SEM

Z. Sun, G. Song, T. Sisneros, B. Clausen, C. Pu, L. Li, Y. Gao, and P. K. Liaw, Scientific Reports 6 (2016) 23137.

G. Song, Z. Sun, J. D. Poplawsky, Y. Gao, c, P. K. Liaw, Acta Mater., 127 (2017) 1-16.

M. J. S. Rawlings, C. H. Liebscher, M. Asta, D. C. Dunand, Acta Mater., 128 (2017) 103-112.

Current Progress-First-principles Calculations

- Elastic properties (single-crystal C_{ij} of α-Fe and $B2$-NiAl) are known.
- But, those of $L2_1$-Ni_2TiAl are not known. Yet, they are important for structure-property relations and modeling.
- Present study: First-principles calculations of C_{ij} of Ni_2TiAl
- $L2_1$-Ni_2TiAl is a cubic phase: Three C_{ij} (C_{11}, C_{12}, and C_{44})
- Born stability criterion is satisfied:
  $C_{11} > 0$; $C_{44} > 0$; $C_{11} > C_{12}$ and $C_{11} + 2C_{12} > 0$

Current Progress - First-principles Calculations (Cont'd)

Fe				
C_{ij} (10^{10} N/m^2)				
	Energy-strain	**Stress-Strain**	**Experimental Results**	**Previous Calculation**
C_{11}	**26.437**	**28.873**	**24.31**[1]	**27.9**[2]
C_{12}	**13.510**	**14.266**	**13.81**[1]	**14.0**[2]
C_{44}	**9.121**	**9.176**	**12.19**[1]	**9.9**[2]

[1] J. Rayne, B. Chandrasekhar. Elastic constants of iron from 4.2 to 300 K, Physical Review 122 (1961) 1714.

[2] T. Davenport, L. Zhou, J. Trivisonno. Ultrasonic and atomic force studies of the martensitic transformation induced by temperature and uniaxial stress in NiAl alloys, Phys. Rev. B 59 (1999) 3421.

Current Progress - First-principles Calculations (Cont'd)

B2-NiAl				
C_{ij} (10^{10} N/m^2)				
	Energy-strain	**Stress-Strain**	**Experimental Results**	**Previous Calculation**
C_{11}	**20.730**	**20.844**	**20.67**[4]	**23.3**[3], **23.6**[5], **17.23**[6]
C_{12}	**13.548**	**13.571**	**13.54**[4]	**17.3**[3], **16.7**[5], **14.6**[6]
C_{44}	**11.618**	**11.720**	**11.68**[4]	**11.5**[3], **14.0**[5], **10.03**[6]

[3] G. Guo, H. Wang. Gradient-corrected density functional calculation of elastic constants of Fe, Co and Ni in bcc, fcc and hcp structures, Chin. J. Phys 38 (2000) 949-961.

[4] X. Huang, I.I. Naumov, K.M. Rabe. Phonon anomalies and elastic constants of cubic NiAl from first principles, Phys. Rev. B 70 (2004) 064301.

[5] H. Fu, D. Li, F. Peng, T. Gao, X. Cheng. Ab initio calculations of elastic constants and thermodynamic properties of NiAl under high pressures, Computational Materials Science 44 (2008) 774-778.

[6] J.F. Nye. Physical properties of crystals: their representation by tensors and matrices, Oxford university press, 1985.

Current Progress - First-principles Calculations (Cont'd)

$L2_1$-Ni_2TiAl				
C_{ij} (10^{10} N/m^2)				
	Energy-strain	**Stress-Strain**	**Experimental Results**	**Previous Calculation**
C_{11}	**21.169**	**22.459**	**None**	**None**
C_{12}	**14.347**	**13.725**	**None**	**None**
C_{44}	**8.139**	**9.192**	**None**	**None**

Current Progress - CALPHAD Calculations

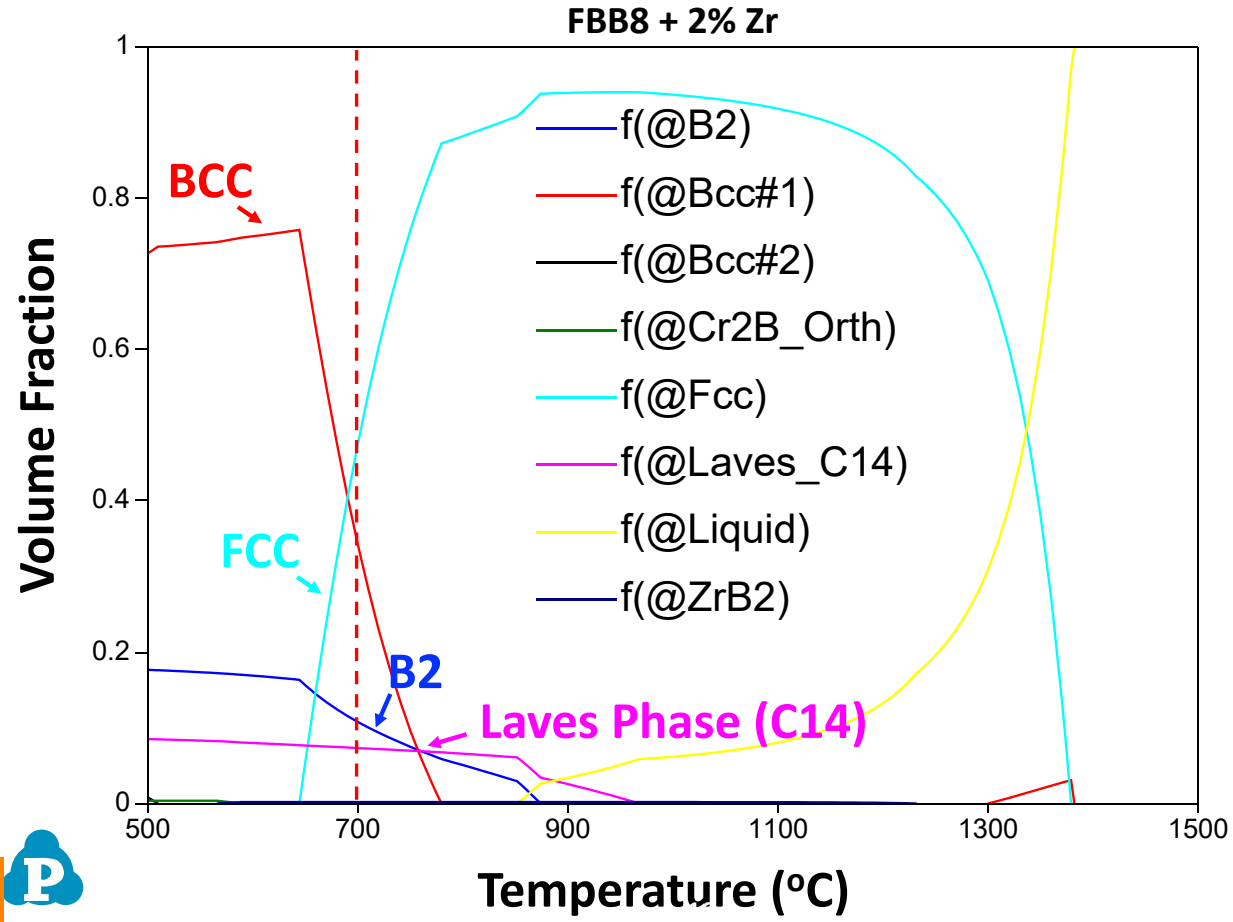

Current Progress - CALPHAD Calculations (Cont'd)

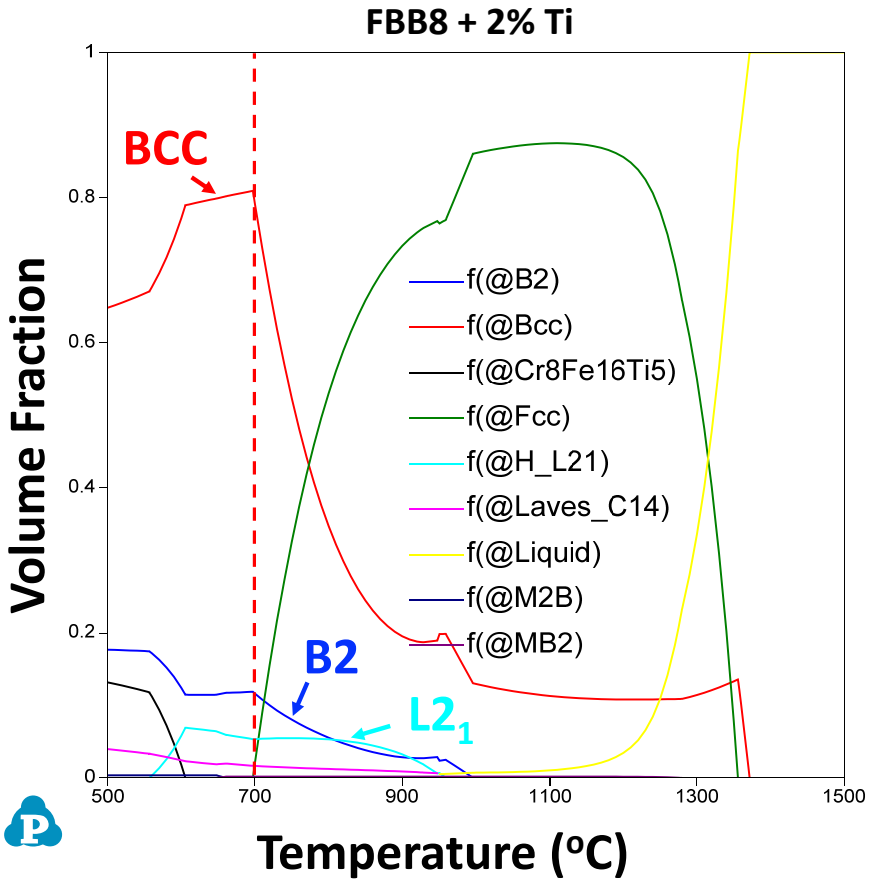

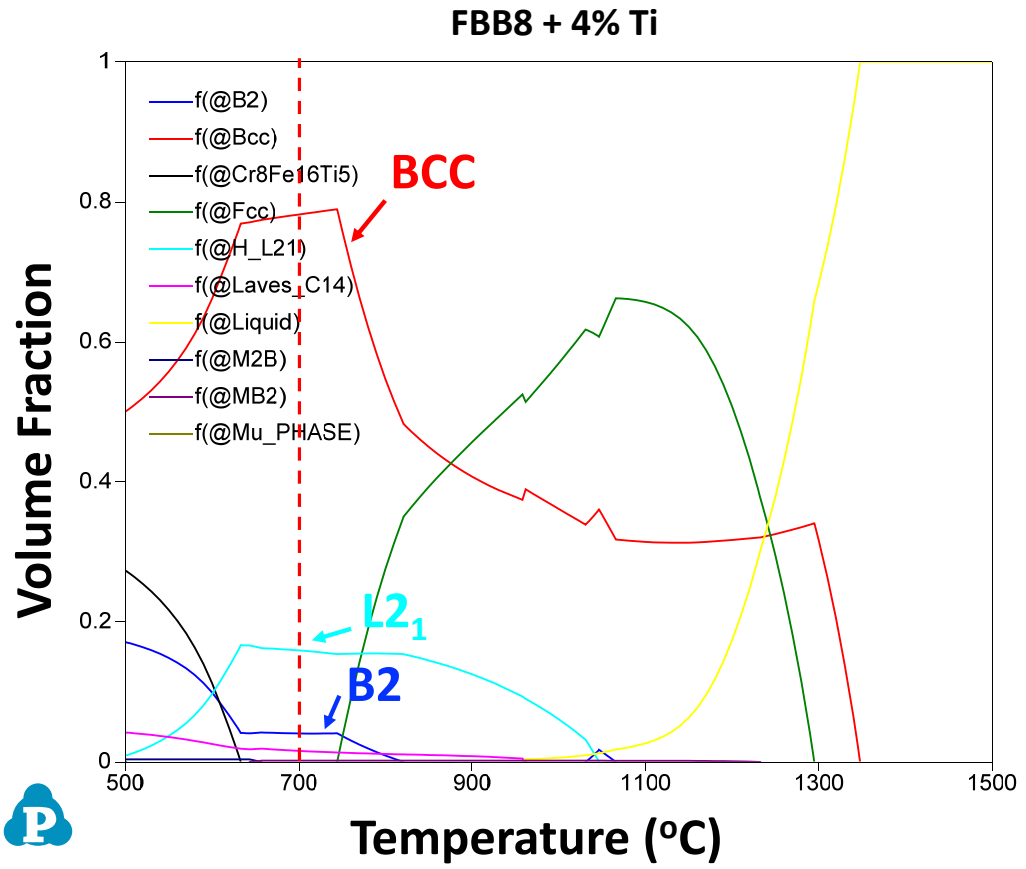

Current Progress - Microstructural Characterization with LEAP

FBB8

Average concentrations in precipitates

Ti ↑ → Fe ↑; Ni, Al↓

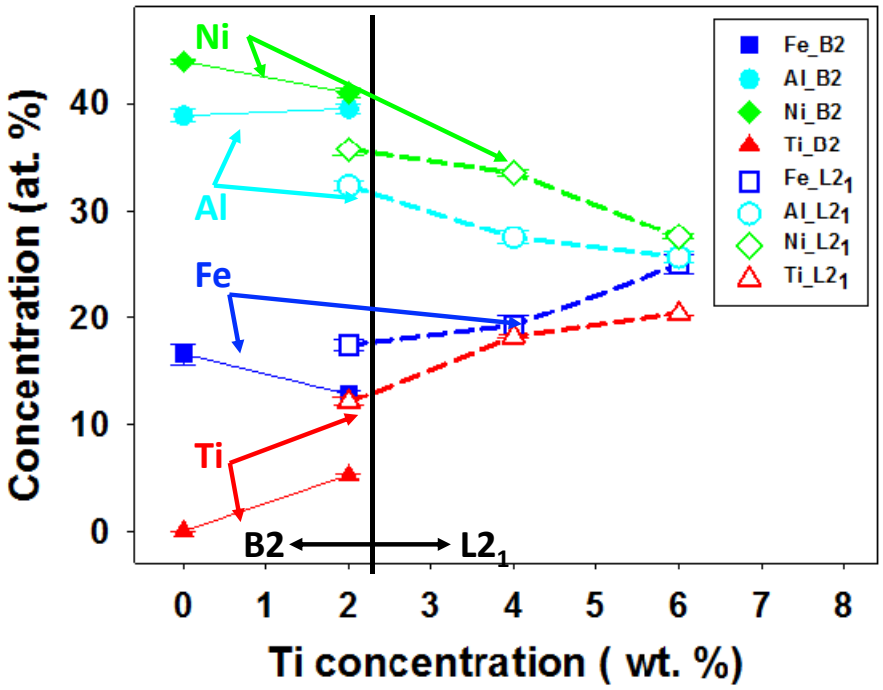

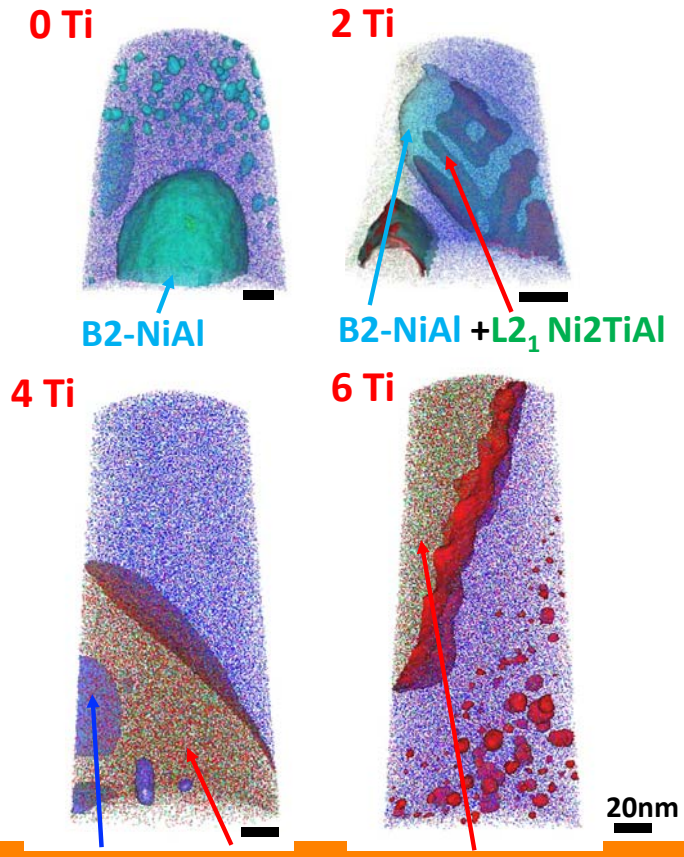

Current Progress - Microstructural Characterization with LEAP (Cont'd)

2Ti

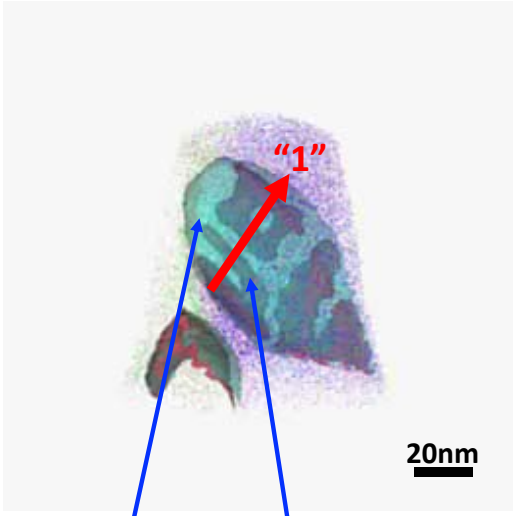

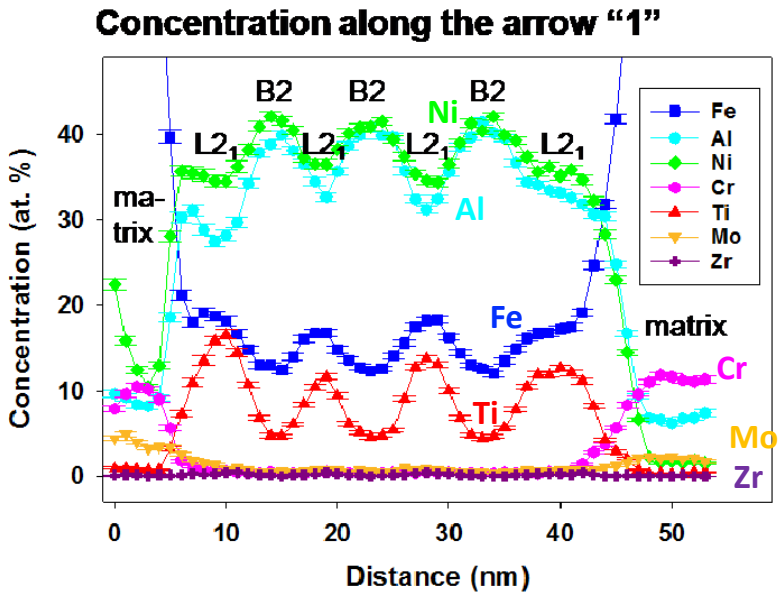

- A chemical analysis along the red arrow shows that the chemical distribution of the precipitates, B2 and $L2_1$ phase are formed staggeredly.

Current Progress - Microstructural Characterization with LEAP (Cont'd)

4Ti

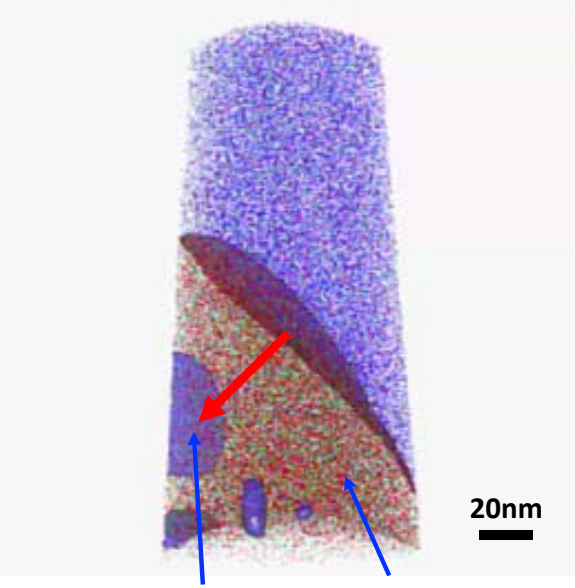

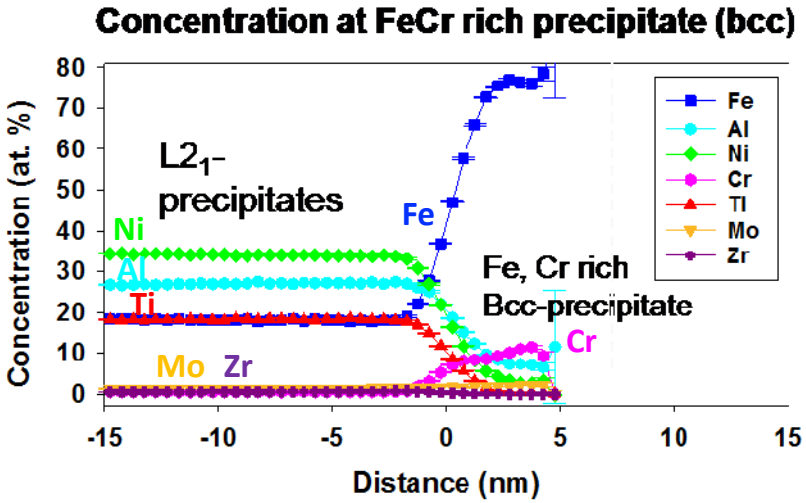

- A chemical analysis along the red arrow shows that the chemical distributions of the precipitates, B2 and $L2_1$ phases are formed staggeredly.

Current Progress - Microstructural Characterization on FBB8 + 2 wt.% Hf

- The FBB8 + 2 wt.% Hf alloy shows a complicated microstructure on SEM images. At least, two kinds of precipitates are present.

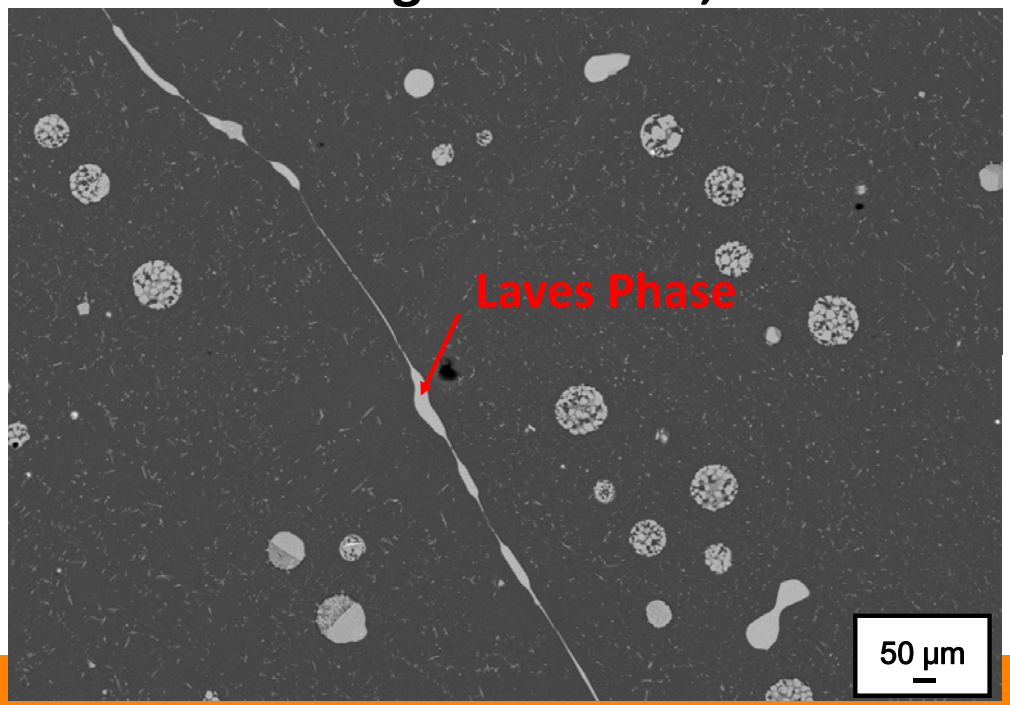

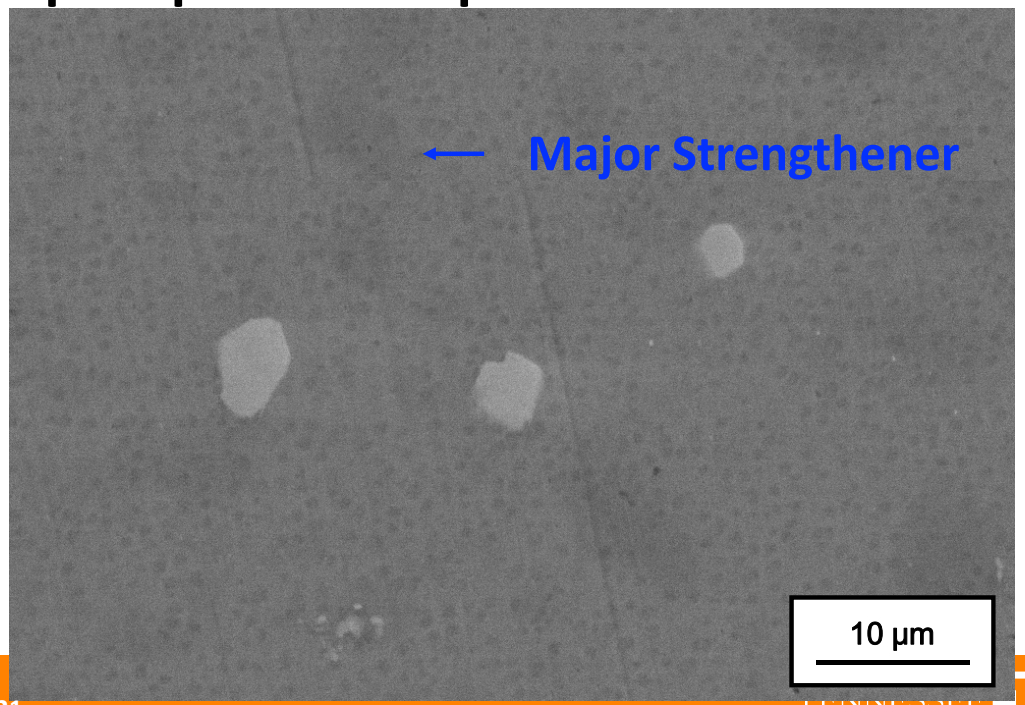

Current Progress - Microstructural Characterization on FBB8 + 2 wt.% Zr

- Microstructure, very similar to FBB8 + 2 wt.% Hf alloy.

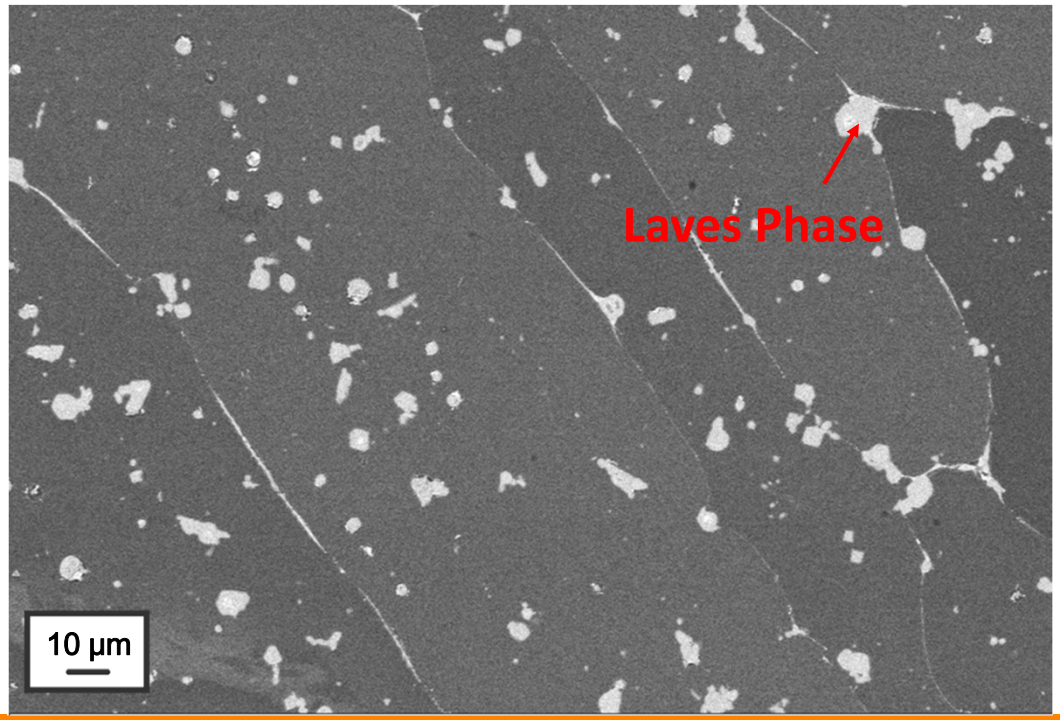

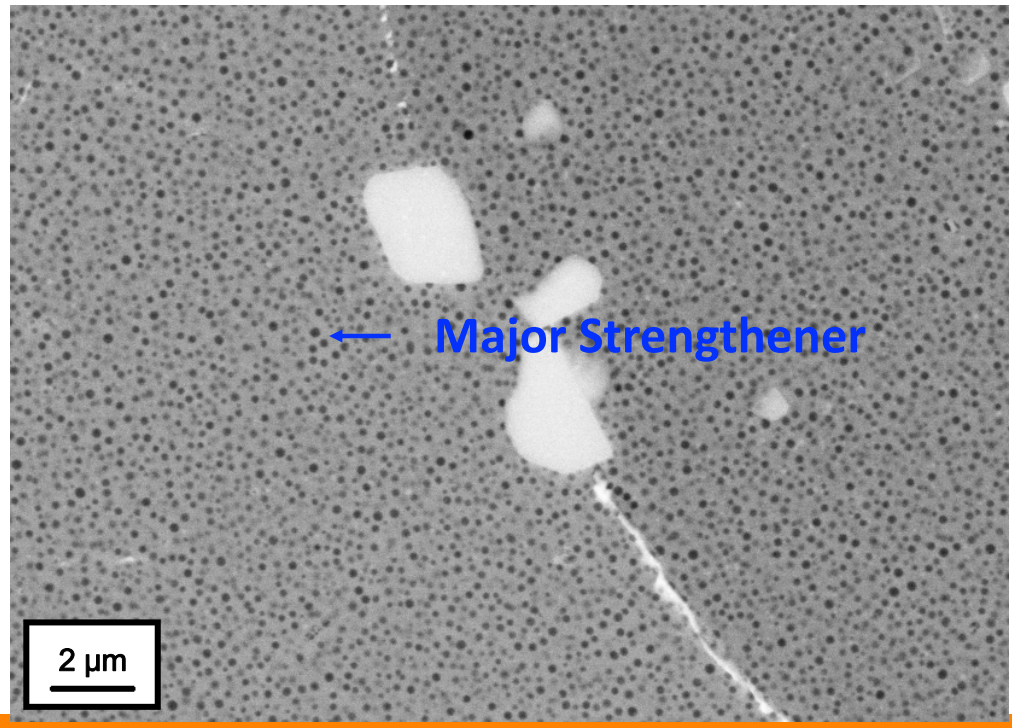

Current Progress - Microstructural Characterization on FBB8 + 1 wt.% Hf-1 wt.% Ti

- 1 wt.% Hf forms high Z-contrast secondary phase along the grain boundaries, and 1 wt.% Ti does not enough to form the $L2_1$ phase.

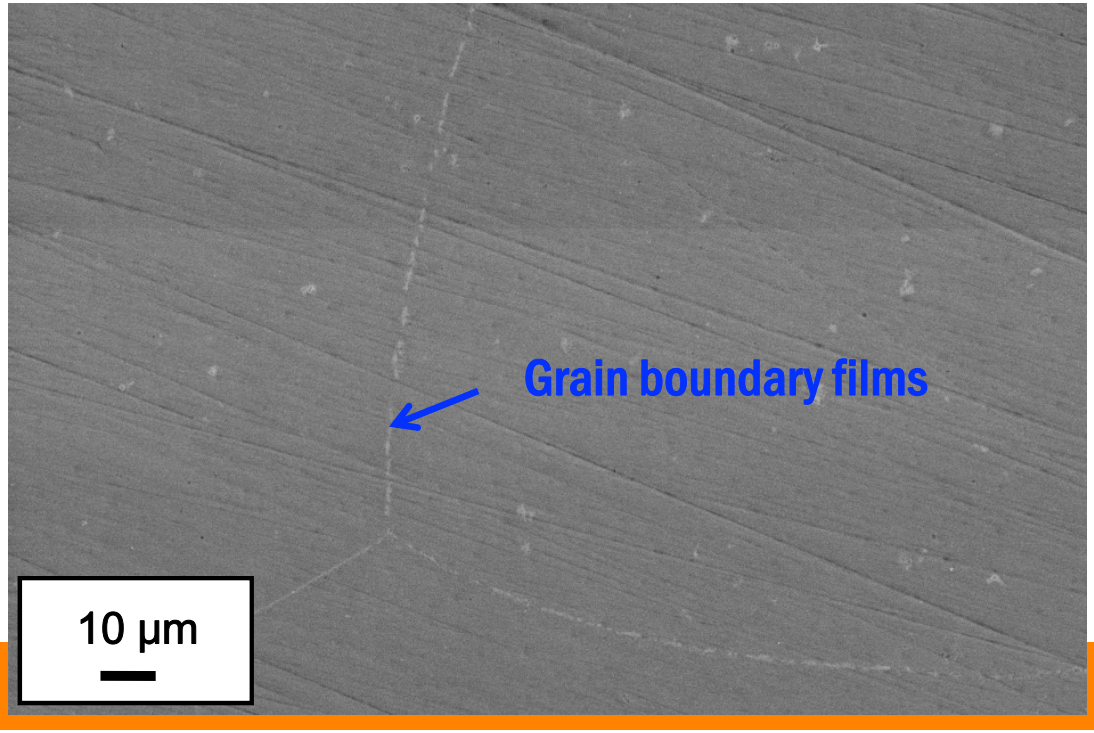

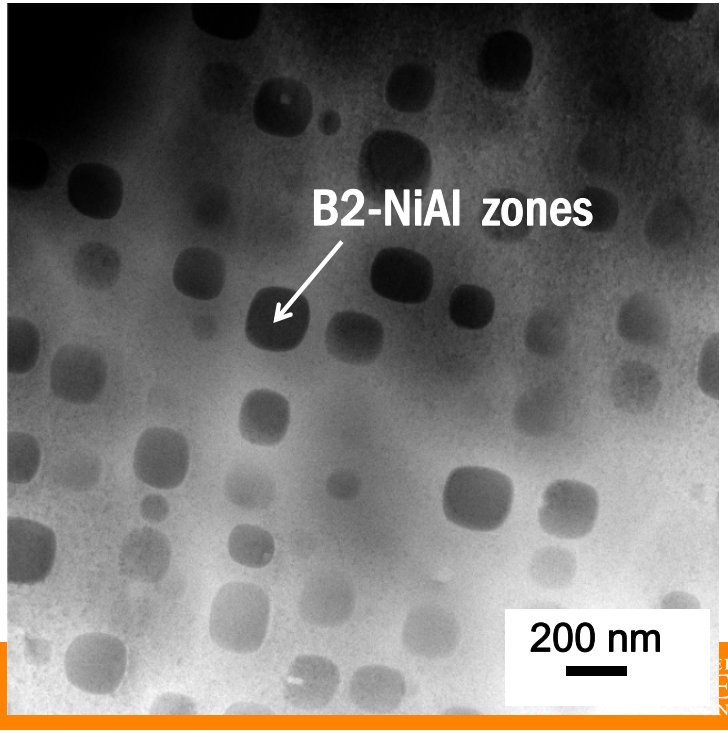

Current Progress - Microstructural Characterization on FBB8 + 0.5 wt.% Hf - 1.5 wt.% Ti

- Very clean microstructure, compared to FBB8 + 2 wt.% Hf and FBB8 + 2 wt.% Zr.

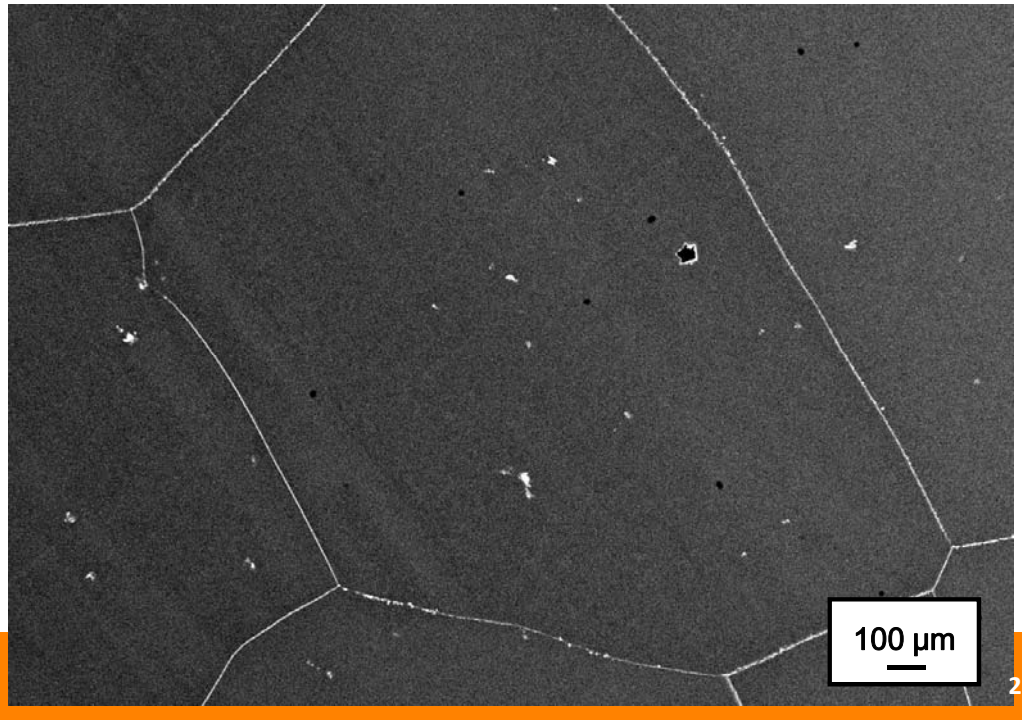

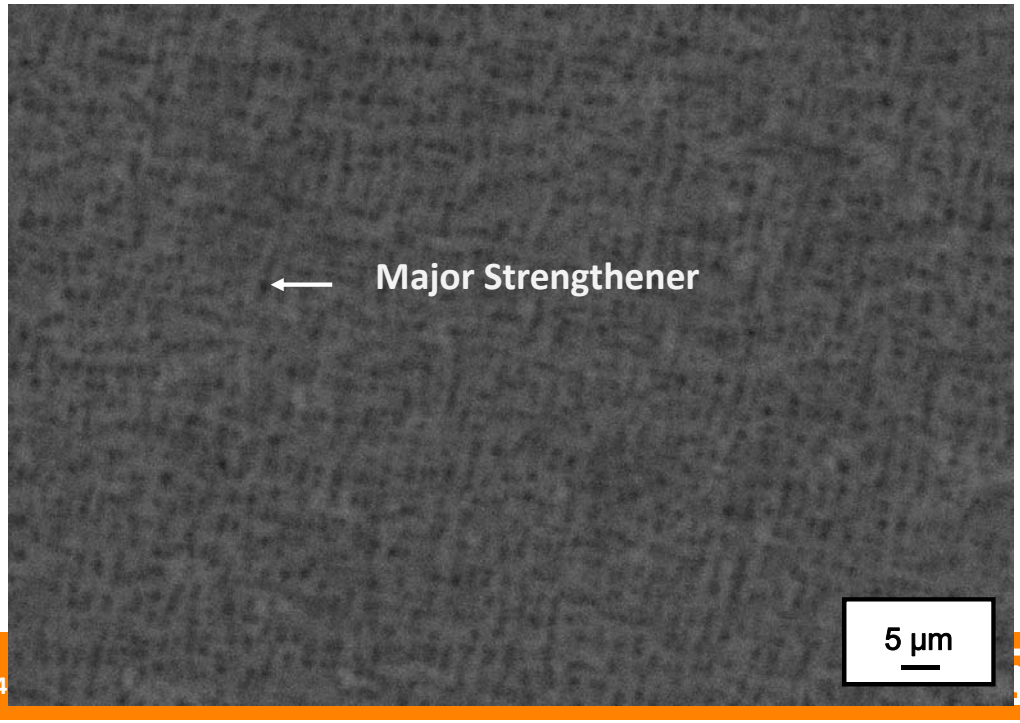

Current Progress - Creep Tests

- Creep tests on FBB8 + 2 wt.% Hf showed no creep-resistance enhancement. Its creep-resistance is similar to FBB8.

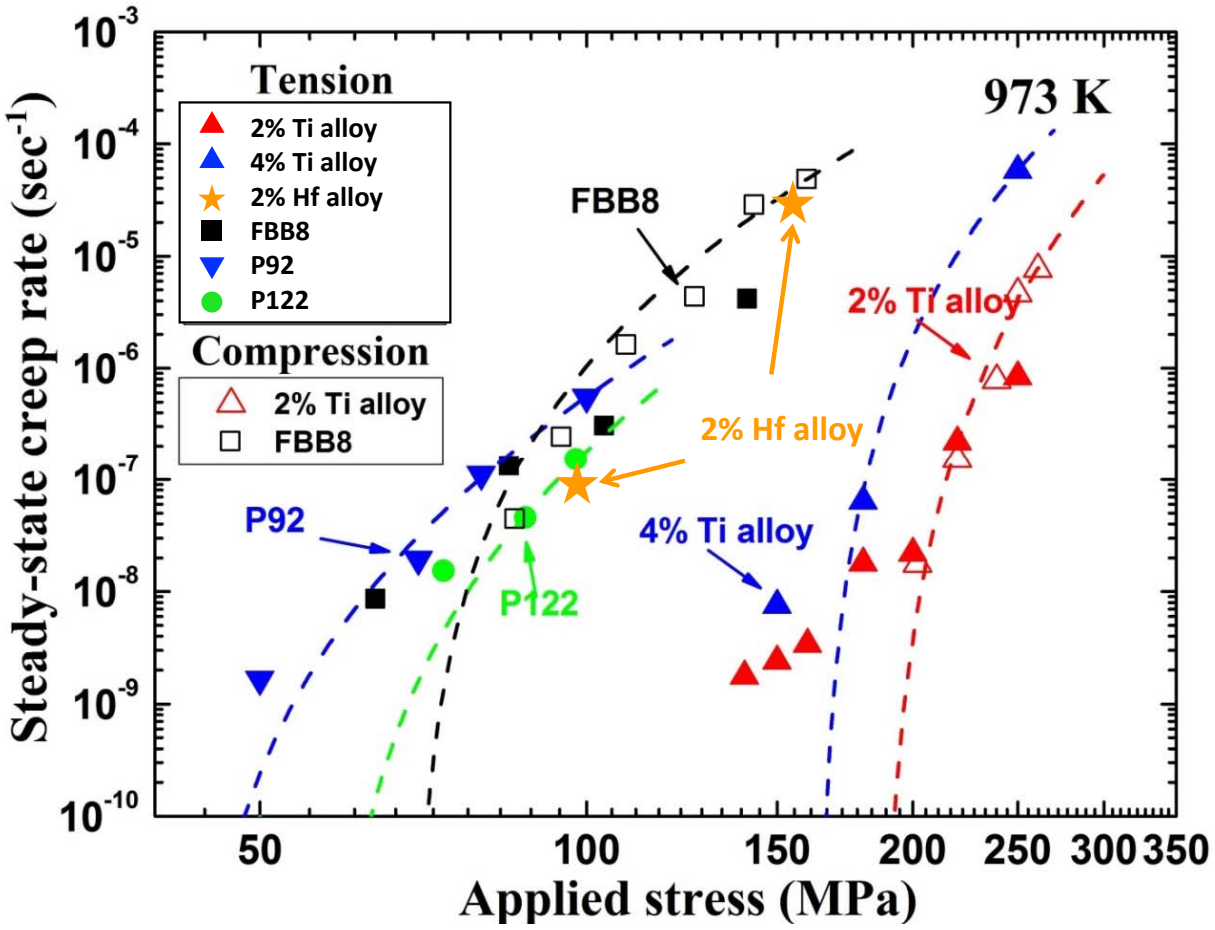

G. Song, Z. Sun, L. Li, X. Xu, M. Rawlings, C.H. Liebscher, B. Clausen, J. Poplawsky, D.N. Leonard, S. Huang, Z. Teng, C.T. Liu, M.D. Asta, Y. Gao, D.C. Dunand, G. Ghosh, M. Chen, M.E. Fine, and P.K. Liaw, Scientific Report, 5 (2015) 16327.

Creep Behavior

Aging temperature and time effects on creep resistance

Materials: Fe-2Ti-6.5Al-10Cr-10Ni-3.4Mo-0.25Zr-0.005B (wt.%)

Homogenized at 1,200 °C for 0.5 h, then:

- **aged: 700, 740, 780 °C for 100 h**
- **creep test: at 700 °C under stress ranging from 70 – 270 MPa**
- **added condition for comparison: aged 700 °C for 900 hr**

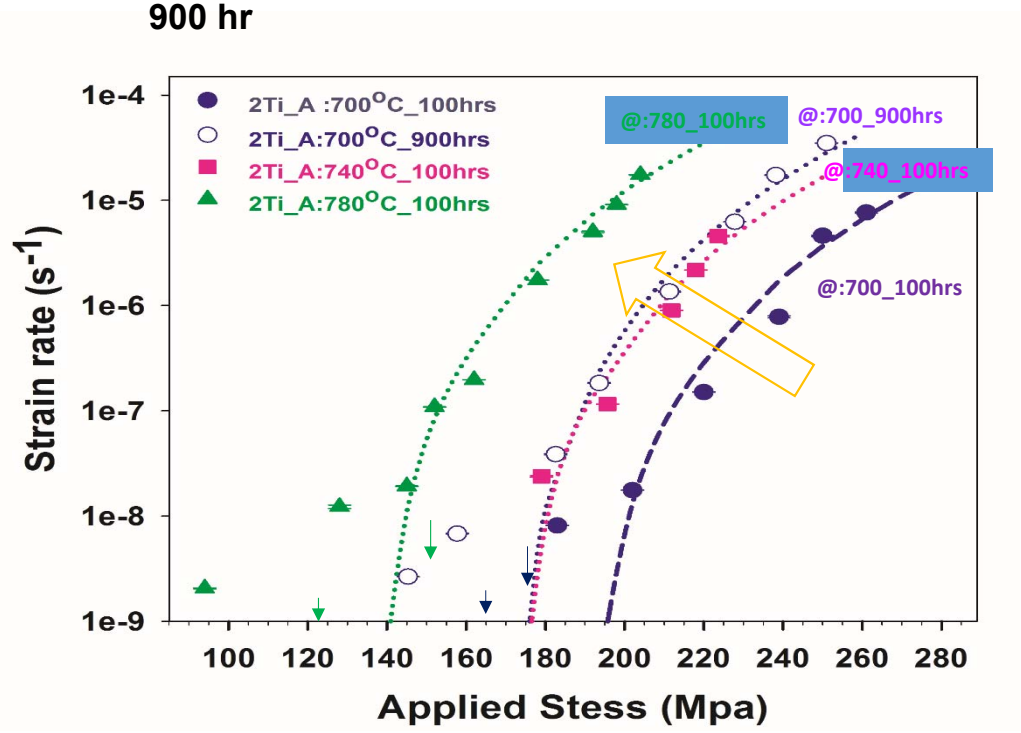

Creep strain rate vs. applied stress

$$\dot{\varepsilon}_s = A\frac{\mu bD}{kT}\left(\frac{\sigma-\sigma_{th}}{\mu}\right)^n$$

where A is a constant, μ is the shear modulus, D is the effective diffusion coefficient, k is the Boltzmann constant, T is the temperature, σ_{th} is the threshold stress, and n is the creep-stress exponent

Threshold stress of the FBB8+2Ti ferritic alloy with different aging temperatures/times

Sample tested	Threshold stress (MPa)
Aged @ 700°C for 100hr Tested:700°C	179
Aged @ 740°C for 100hr	168.2
Aged @ 780°C for 100hr	135.5
Aged @ 700°C for 900hr	169.1

Manuscript in preparation, NU

Papers, Presentations, and Awards

- **Papers**

1. Z. K. Teng, M. K. Miller, G. Ghosh, C. T. Liu, S. Huang, K. F. Russel, M. E. Fine, and P. K. Liaw, Scripta Materialia, 2010;63:61.
2. S. Huang, D. L. Worthington, M. Asta, V. Ozolins, G. Ghosh, and P. K. Liaw, Acta Materialia, 2010;58:1982.
3. S. Huang, B. Clausen, D. Brown, Z. K. Teng, Y. F. Gao, and P. K. Liaw, Metallurgical and Materials Transactions A, 2012;43:1497.
4. Z. K. Teng, F. Zhang, M. K. Miller, C. T. Liu, S. Huang, Y. T. Chou, R. H. Tien, Y. A. Chang, and P. K. Liaw, Materials Letters, 2012;71:36.
5. Z. K. Teng, G. Ghosh, M. K. Miller, S. Huang, B. Clausen, D. W. Brown, and P. K. Liaw. Acta Mater. 2012;60:5362.
6. Z. K. Teng, C. T. Liu, M. K. Miller, G. Ghosh, E. A. Kenik, S. Huang, and P. K. Liaw, Materials Science and Engineering A, 2012;541:22.

Papers, Presentations, and Awards (Cont'd)

7. H. Ding, S. Huang, G. Ghosh, P. K. Liaw, and M. Asta, Scripta Mater. 2012;67:732.

8. S. Huang, G. Ghosh, X. Li, J. Ilavsky, Z. K. Teng, and P. K. Liaw, Metallurgical and Materials Transactions A. 2012;43:3423.

9. C. H. Liebscher, V. Radmilovic, U. Dahmen, M. Asta and G. Ghosh, Journal of Materials Science, 2013;48:2067.

10. Z. Sun, C. H. Liebscher, S. Huang, Z. Teng, G. Song, G. Wang, M. Asta, M. Rawlings, M. E. Fine, and P. K. Liaw, Scripta Materialia, 2013;68:384.

11. H. Ding, V. I. Razumovsky, and M. Asta, Self Diffusion Anomaly in Ferromagnetic Metals: A Density-Functional-Theory Investigation of Magnetically Ordered and Disordered Fe and Co, Acta Mater., 70 (2014) 130-136.

12. H. Ding, V.I. Razumovskiy, M. Asta, Acta Mater., 70 (2014) 130-136.

13. S. Huang, Y. Gao, K. An, L. Zheng, W. Wu, Z. Teng, and P.K. Liaw, Acta Mater., 83 (2015) 137-148.

Papers, Presentations, and Awards (Cont'd)

14. Z. Sun, G. Song, J. Ilavsky, and P.K. Liaw, Materials Research Letters, (2015) 128-134.
15. C.H. Liebscher, V.R. Radmilović, U. Dahmen, N.Q. Vo, D.C. Dunand, M. Asta, and G. Ghosh, Acta Mater., 92 (2015) 220-232.
16. G. Song, Z. Sun, L. Li, X. Xu, M. Rawlings, C.H. Liebscher, B. Clausen, J. Poplawsky, D.N. Leonard, S. Huang, Z. Teng, C.T. Liu, M.D. Asta, Y. Gao, D.C. Dunand, G. Ghosh, M. Chen, M.E. Fine, and P.K. Liaw, Scientific Report, 5 (2015) 16327.
17. Z. Sun , G. Song , J. Ilavsky , G. Ghosh, and P.K. Liaw, Scientific Report, 5 (2015) 16081.
18. Z. Sun, G. Song, T. Sisneros, B. Clausen, C. Pu, L. Li, Y. Gao, and P. K. Liaw, Scientific Reports 6 (2016) 23137.
19. G. Song, Z. Sun, J. D. Poplawsky, Y. Gao, and P. K. Liaw, Acta Mater., 127 (2017) 1-16.
20. G. Song, Z. Sun, , J. D. Poplawsky, X. Xu, M. Chen, and P. K. Liaw, Journal of Alloys and Compounds 706, (2017) 584–588.

Papers, Presentations, and Awards (Cont'd)

21. G. Song, Z. Sun, B. Clausen, and P. K. Liaw, Journal of Alloys and Compounds 693, (2017) 921–928.

22. M. J. S. Rawlings, C. H. Liebscher, M. Asta, and D. C. Dunand, Acta Mater., 128 (2017) 103-112.

Papers, Presentations, and Awards (Cont'd)

- **Presentations**

1. Z. K. Teng, F. Zhang, M. K. Miller, C. T. Liu, A. Y. Chuang, S. Y. Huang, R. H. Tien, Y. T. Chou, and P. K. Liaw. 2011 TMS Meeting, San Diego, 02/27 – 03/04.

2. S. Y. Huang, B. Clausen, D. Brown, Z. Teng, G. Ghosh, M. Fine, and P. K. Liaw, 2011 TMS Meeting, San Diego, 02/27 – 03/04.

3. P. K. Liaw, Z. Teng, S. Huang, C. T. Liu, M. E. Fine, G. Ghosh, M. D. Asta, and G. Wang, The Annual University Coal Research/Historically Black Colleges and Universities and Other Minority Institutions Conference, Pittsburgh, Pennsylvania, 06/07 – 06/08, 2011

4. S. Huang, Y. F. Gao, K. An, W. Wu, L. Zheng, M. Rawlings, D. Dunand, and P. K. Liaw, 2012 TMS Meeting, Orlando, Florida , 03/11 – 03/15.

5. P. K. Liaw, M. D. Asta, D. C. Dunand, M. E. Fine, G. Ghosh, and C. T. Liu, National Energy Technology Laboratory, Pittsburgh, Pennsylvania, 04/18, 2012

Papers, Presentations, and Awards (Cont'd)

6. C. H. Liebscher, V. Radmilovic, U. Dahmen, M. Asta, and G. Gosh, Microscopy & Microanalysis 2012 Meeting, Phoenix, Arizona, 07/29 - 08/02

7. C. H. Liebscher, V. Radmilovic, U. Dahmen, M. Asta, and G. Gosh, Materials Science and Technology 2012 Meeting, Pittsburgh, Pennsylvania, 08/07 - 08/11

8. H. Ding, S. Huang, G. Ghosh, P. K. Liaw, and M. Asta, Materials Science and Technology 2012 Meeting, Pittsburgh, Pennsylvania, 08/07 - 08/11

9. Z. Sun, G. Song, Z. Teng, G. Ghosh, and P. K. Liaw , 2012 MRS Fall Meeting & Exhibit, Boston, 11/25 – 11/30

10. P. K. Liaw, M. Asta, D, Dunand, M. Fine, G. Ghosh, C. Liu, H. Ding, S. Huang, M. Rawlings, Z. Sun, G. Song, Z. Teng, G. Wang, and C. Liebscher, 2013 TMS Meeting , San Antonio, Texas, 03/03 – 03/07

11. Z. Sun, S. Huang, Z. Teng, G. Song, G. Wang, and P. K. Liaw, 2013 TMS Meeting, San Antonio, Texas, 03/03 – 03/09

Papers, Presentations, and Awards (Cont'd)

12. G. Song, Z. Sun, G. Wang, H. Ding, C. Liebscher, M. D. Asta, G. Ghosh, D. C. Dunand, M. Rawlings, N. Q Vo, and P. K. Liaw, 2015 TMS Meeting, Orlando, Florida, 3/15 – 3/19

13. Z. Sun, G. Song, J. Ilavsky, and P. K. Liaw, 2015 Materials Science & Technology Conference (MS&T), Columbus, Ohio, 10/4 – 10/8

14. G. Song, Z. Sun, L. Li, X. Xu, M. Rawlings, C. Liebscher, B. Clausen, J. Poplawsky, D. Leonard, S. Huang, Z. Teng, C. Liu, M. Asta, Y. Gao, D. Dunand, G. Ghosh, M. Chen, M. Fine, and P. K. Liaw, 2015 Materials Science & Technology Conference (MS&T), Columbus, Ohio, 10/4 – 10/8

15. G. Song, Z. Sun, D. Dunand, M. Rawlings, G. Ghosh, and P. K. Liaw, 2016 TMS Meeting, Nashville, Tennessee, 02/14 – 02/18

16. G. Song, Y. Gao, Z. Sun, J. Poplawsky, and P. K. Liaw , 2016 TMS Meeting, Nashville, Tennessee, 02/14 – 02/18

17. Z. Sun, G. Song, J. Ilavsky, G. Ghosh, and P. K. Liaw, 2016 TMS Meeting, Nashville, Tennessee, 02/14 – 02/18

Papers, Presentations, and Awards (Cont'd)

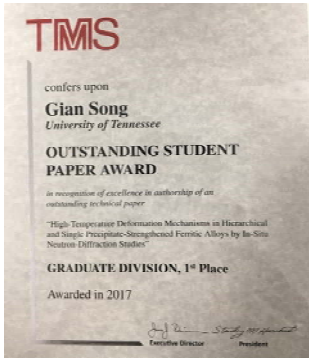
TMS

confers upon

Gian Song

University of Tennessee

OUTSTANDING STUDENT PAPER AWARD

in recognition of excellence in authorship of an outstanding technical paper

"High-Temperature Deformation Mechanisms on Hierarchical and Single Precipitate-Strengthened Ferritic Alloys by In-Situ Neutron-Diffraction Studies"

GRADUATE DIVISION, 1st Place

Awarded in 2017

Executive Director President

- **Awards**
  1. **Zhiqian Sun, TMS Best Paper Contest – Graduate Division – First Place, TMS 2016 Annual Meeting & Exhibition, Feb. 14-18, 2016, Nashville, Tennessee**
  2. **Gian Song, TMS Best Paper Contest – Graduate Division – Second Place, TMS 2016 Annual Meeting & Exhibition, Feb. 14-18, 2016, Nashville, Tennessee**
  3. **Gian Song, TMS Best Paper Contest – Graduate Division – First Place, TMS 2017 Annual Meeting & Exhibition, Feb. 26-Mar. 2, 2017, San Diego, California**

Summaries and Current Status

- Single-crystal elastic constants (C_{ij}) are calculated using the first-principles method in a hierarchical microstructure.

- Calculated results show a good agreement with experimental data, when available. As of now, there is no experimental C_{ij} data of $L2_1$-Ni_2TiAl. Thus, present calculations fill an important knowledge gap.

- CALPHAD calculations help in predicting microstructures in alloy systems.

Summaries and Current Status (Cont'd)

- Current investigations on the FBB8 + Hf and FBB8 + Zr alloy systems show poor tendency to form $L2_1$ phase, which leads to no enhancement on creep-resistance.

Zr

- Similar microstructure as FBB8 + 2% Hf.
- Disarray
- Segregations along grain boundary and within grains.
- Strengthener: B2 phase.

Hf

- Disarray.
- Segregations along grain boundary and within grains.
- Strengthener: B2 phase.

Ti

- Uniform.
- Limited amount of segregation.
- Strengthener: B2 or $L2_1$ phase.

Future Plan

- We will focus on the FBB8 + Ti alloy system to determine the optimum Ti content in order to achieve greatest creep resistance.

- FBB8 + 2.5 wt.% Ti, FBB8 + 3 wt.% Ti, and FBB8 + 3.5 wt.% Ti alloys have been fabricated. SEM, TEM, LEAP, and creep tests are in progress and will be completed in the near future.

- In-situ neutron experiments will be performed, in order to characterize the microscopic mechanical information.

-The End-

Any Questions?

Current Progress - First-principles Calculations (Cont'd)

- **Directional property: Young's modulus**

G. Ghosh and P.K. Liaw, in preparation, 2017.

G. Ghosh, *AIP Advances*, 5, 087102 (2015)

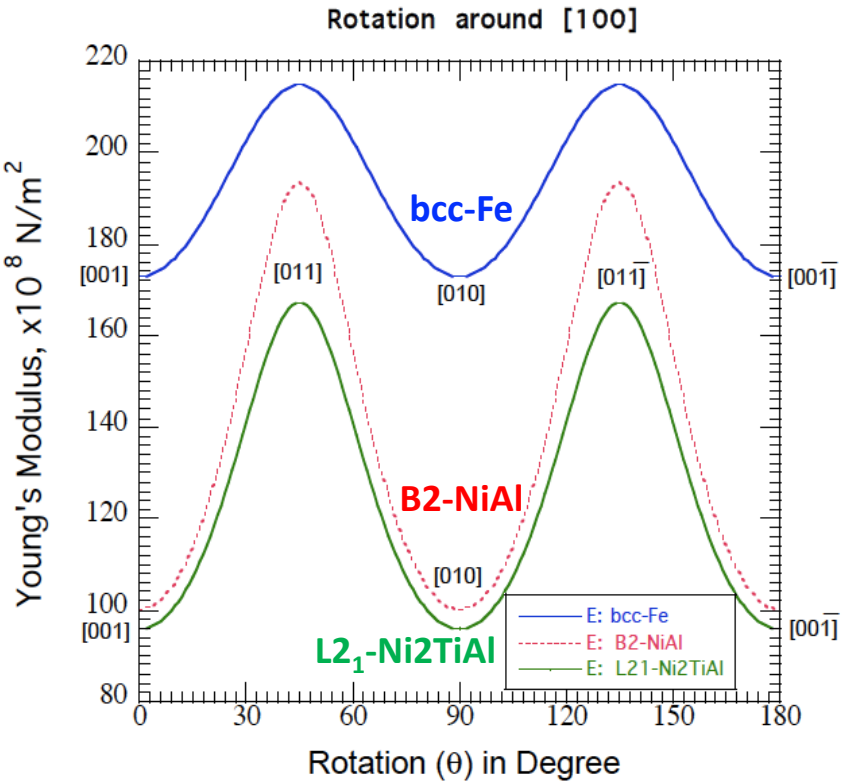

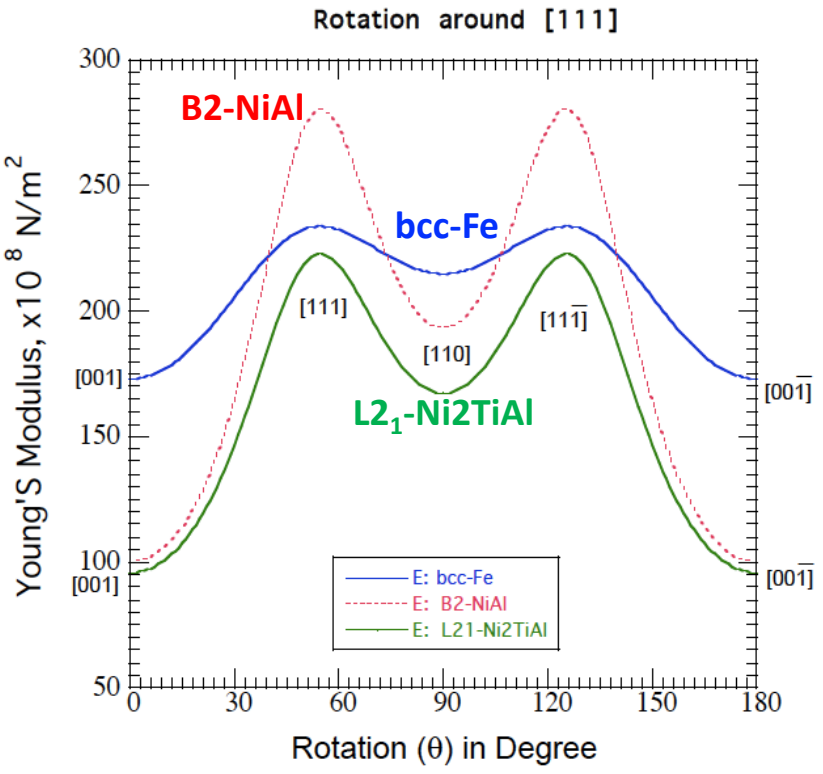

Current Progress - First-principles Calculations (Cont'd)

- **Directional property: shear modulus**

$$\frac{1}{G} = S_{44}$$
$$= 4S_{11}(l_{11}^2 l_{21}^2 + l_{12}^2 l_{22}^2 + l_{13}^2 l_{31}^2)$$
$$+ 8S_{12}(l_{11}l_{21}l_{12}l_{22} + l_{11}l_{22}l_{13}l_{31}$$
$$+ l_{11}l_{21}l_{13}l_{31})$$
$$+ S_{44}[(l_{11}l_{22} + l_{21}l_{12})^2 + (l_{12}l_{31} + l_{12}l_{13})^2$$
$$+ (l_{11}l_{31} + l_{21}l_{13})^2]$$

- **S_{ij} are elastic compliances, l_{ij} are directional cosine.**

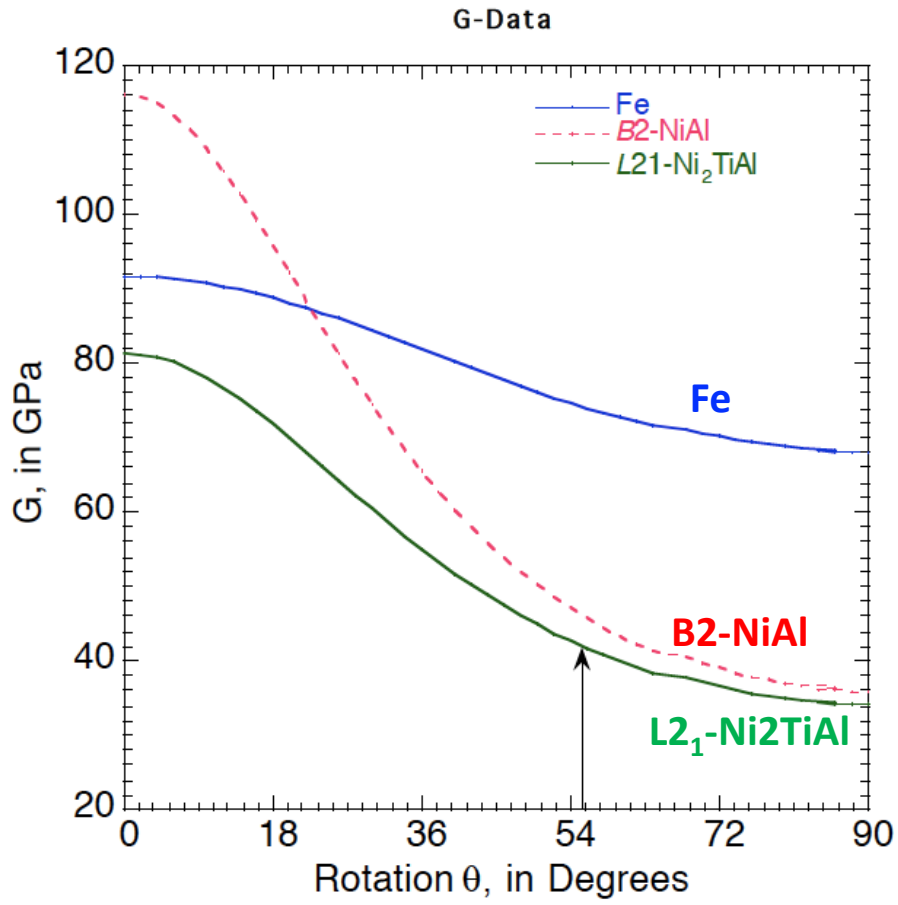

Current Progress - First-principles Calculations (Cont'd)

- From single-crystal C_{ij} data → polycrystalline average ("isotropic property")
- Four distinct methods: (i) Voigt's method, (ii) Reuss' method, and (iii) Hill's method (also called VRH), (iv) Hashin and Shtrikman using variational principles
- In polycrystalline limit, there are only two independent elastic constants: (i) Bulk modulus (B) and (ii) Shear modulus (μ), others. [Young's modulus (E or Y) and Poisson's ratio (ν) are related to B and μ].

Current Progress - First-principle Calculations (Cont'd)

- **Voigt's method: assumes uniform local strain across grains i.e., $\partial\varepsilon_{ij}/\partial x_k = 0$, where ε_{ij} is the strain tensor, and x is the spatial coordinate.**

  →yields upper bound value

- **Reuss' method: assumes uniform local stress across grains i.e., $\partial\sigma_{ij}/\partial x_k = 0$, where σ_{ij} is the stress tensor.**

  →yields lower bound value

- **Hill's or VRH method: usually considers arithmetic, geometric or harmonic mean of Voigt and Reuss values**

$$\mu_{\text{Hill}} = \frac{\mu_{\text{Voigt}} + \mu_{\text{Reuss}}}{2} \text{ or } \sqrt{\mu_{\text{Voigt}}\mu_{\text{Reuss}}}.$$

- **Hashin and Shtrikman method: either stress or strain or both could be the variational quantity(ies) yielding lower and upper bounds of the property.**

Current Progress - First-principle Calculations (Cont'd)

- Calculated isotropic (polycrystalline) elastic properties of $L2_1$-Ni_2TiAl. Bulk, shear and Young's modulus are in GPa

(This study)	Voigt	Ruess	VRH	HS(-)	HS(+)
Bulk Modulus	166.22	166.22	166.22	166.22	166.22
Shear Modulus	66.03	53.88	69.95	59.19	61.51
Young's Modulus	155.49	129.66	163.59	141.09	146.02
Poisson's Ratio	0.324	0.354	0.315	0.341	0.335

Current Progress - Microstructural Characterization on FBB8 + 1 wt.% Hf-1 wt.% Ti

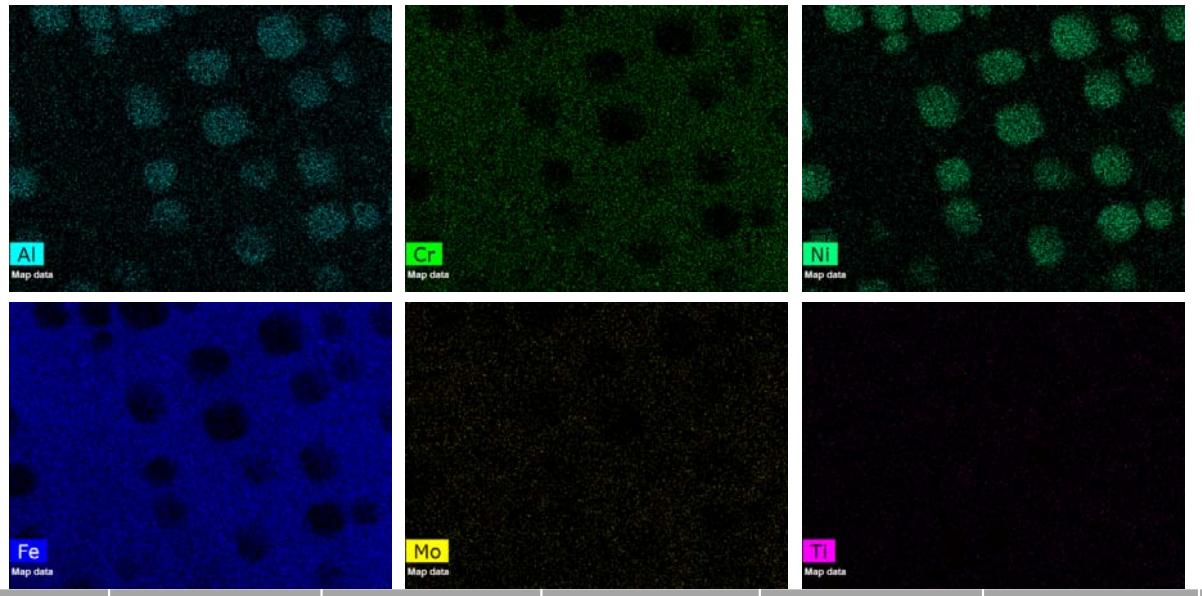

Phase \ Element	Al	Ti	Cr	Fe	Ni	Zr	Mo	Hf
ppt	21.0 ± 0.07	1.8 ± 0.01	1.3 ± 0.03	17.9 ± 0.14	57.2 ± 0.23	0.2 ± 0.04	0.3 ± 0.08	0.3 ± 0.11
Matrix	5.2 ± 0.45	1.3 ± 0.05	12.4 ± 0.13	75.3 ± 0.76	3.3 ± 0.14	0.1 ± 0.05	2.2 ± 0.03	-

Summaries and Current Status

Milestones Designation	Milestone description	Due Date	Revised Due Date	Completion Date
1	First-principles study of thermodynamics	12/31/2015	09/30/2017	03/31/2016
2	First-principles study of elastic properties	12/31/2015	09/30/2017	01/31/2017
3	First-principles study of interfacial properties	12/31/2015	09/30/2017	
4	Design and fabrication of model alloys	12/31/2015	06/30/2017	

Summaries and Current Status (Cont'd)

Milestones Designation	Milestone description	Due Date	Revised Due Date	Completion Date
5	Microstructural characterization (e.g., the precipitate size, volume fraction, morphology, and elemental partitioning between precipitates and the matrix) by HR-AEM, TEM LEAP, and SEM	12/31/2015	06/30/2017	
6	Lattice constants and precipitate volume fraction measurements by XRD and neutron diffraction	12/31/2015	09/30/2017	
7	Coarsening kinetics of NiAl/Ni_2TiAl precipitates in the α-iron matrix investigated by USAXS, TEM, and SEM	12/31/2015	09/30/2017	12/31/2015

Summaries and Current Status (Cont'd)

Milestones Designation	Milestone description	Due Date	Revised Due Date	Completion Date
8	Mechanical properties of model alloys (e.g., compression, tension, hardness tests)	12/31/2015	09/30/2017	
9	Systematical creep study on model alloys	12/31/2015	09/30/2017	
10	Dislocation structures of crept specimens by TEM and STEM	12/31/2015	09/30/2017	
11	In-situ creep study on model alloys under neutron diffraction	12/31/2015	09/30/2017	12/31/2015
12	Dislocation-dynamics simulations of creep resistance	12/31/2015	06/30/2017	12/31/2015

Summaries and Current Status (Cont'd)

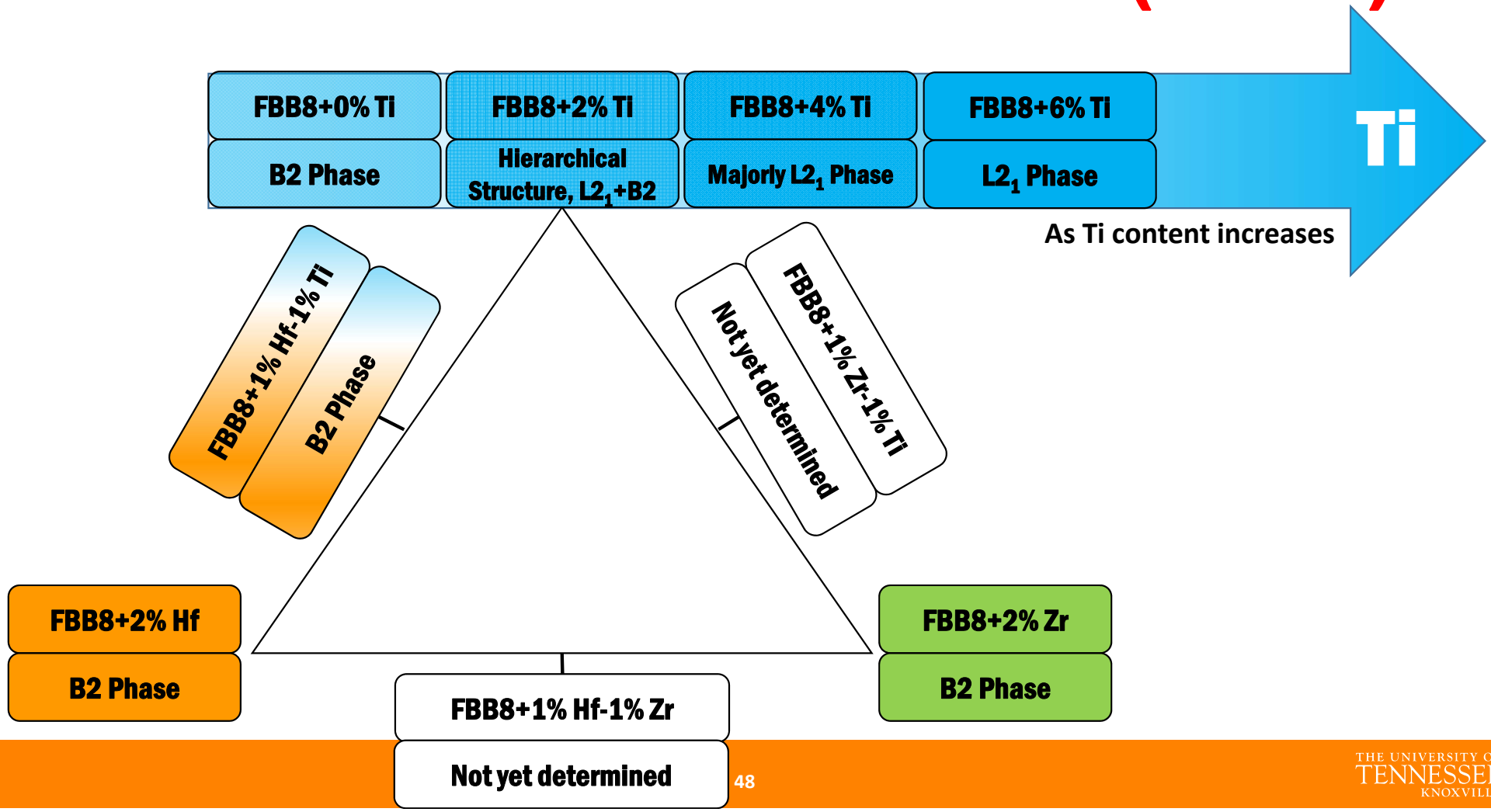

Technical Background of the Project (Cont'd)

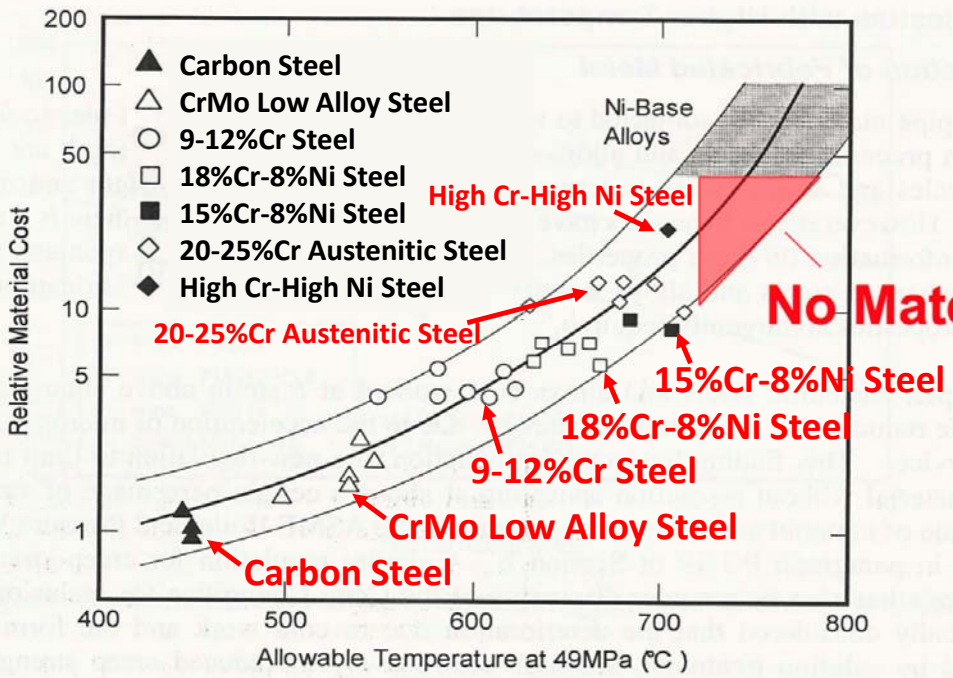

Fig. 7 Relation between allowable metal temperature at the allowable stress of 49MPa and the relative material cost

https://www.netl.doe.gov/File%20Library/Events/2008/fem/Holcomb_pres.pdf

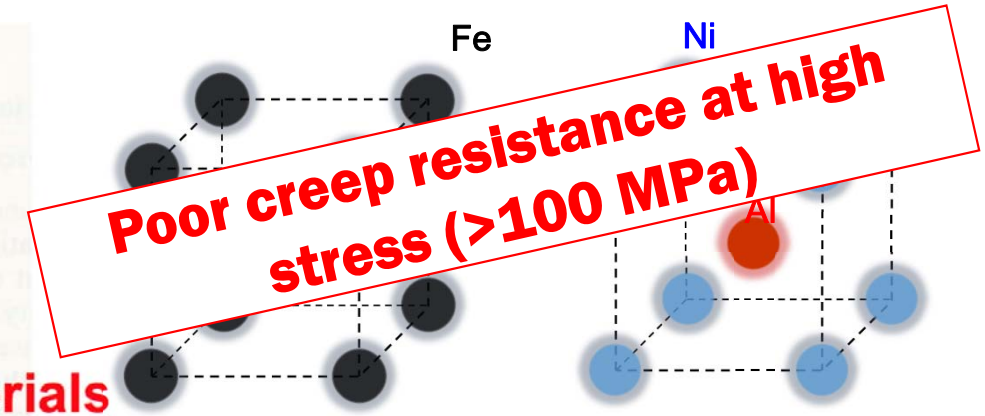

Fe (a phase) NiAl (B2 phase)

FBB8: Fe-6.5Al-10Cr-10Ni-3.4Mo-0.25Zr-0.005B, weight percent (wt.%)

By adding Ti, there will be $L2_1$-Ni_2TiAl formed. The creep strength of $L2_1$ between 753 and 1,000 °C is about three times that of NiAl.

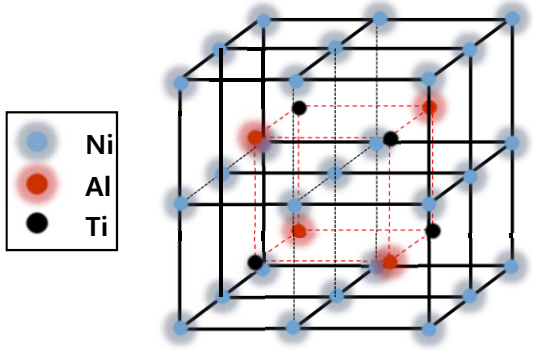

Ni_2TiAl ($L2_1$)

G. Song, Z. Sun, J. D. Poplawsky, Y. Gao, P. K. Liaw, Acta Mater., 127 (2017) 1-16.

G. Song, Z. Sun, L. Li, X. Xu, M. Rawlings, C.H. Liebscher, B. Clausen, J. Poplawsky, D.N. Leonard, S. Huang, Z. Teng, C.T. Liu, M.D. Asta, Y. Gao, D.C. Dunand, G. Ghosh, M. Chen, M.E. Fine, and P.K. Liaw, Scientific Report, 5 (2015) 16327.

Northwestern Univ.

Creep experiment and microstructural analysis for NiAl (B2) and Ni_2TiAl ($L2_1$) precipitate hardened ferritic alloy

Sungil Baik

M. J. S. Rawlings

David C. Dunand

Crept microstructure

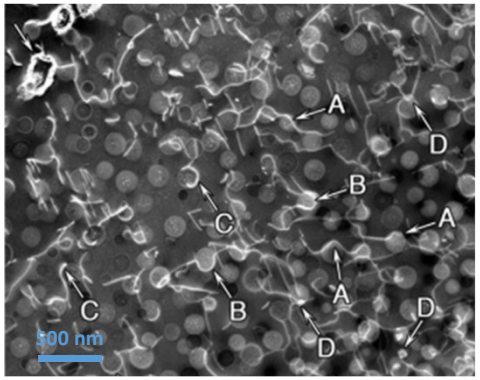

DC-STEM image of FBB8 (0% Ti) after the creep test (after entering a steady-state creep regime)

N.Q. Vo et al. / Acta Materialia 71 (2014)

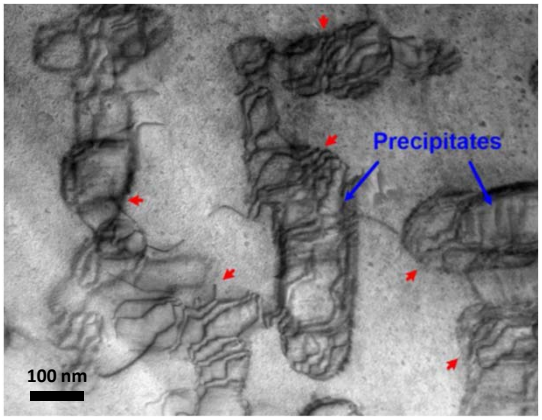

A BF-STEM image of an HPSFA (2wt.% Ti) sample crept at 140 MPa and 973 K, at the creep time of 200 hours

Gian Song et. al., Scientific Reports 2015

Creep mechanisms

(i) Dislocation detachment from precipitates,

(ii) Precipitate shearing,

(iii) Dislocations climbing over precipitates

(iv) Precipitate bypass by Orowan dislocation looping,

What increase the resistance of dislocation precipitate bypass via dislocation loops or climb over coherent hierarchical $L2_1$ (Ni_2TiAl) and B2 (NiAl) precipitate

1. Precipitate size, volume fractions
→ controlled by temperature, aging time
2. Lattice parameter mismatches (structure change (B2→$L2_1$)
→ controlled by Ti concentration changes

Dislocation dynamics (DD) simulation

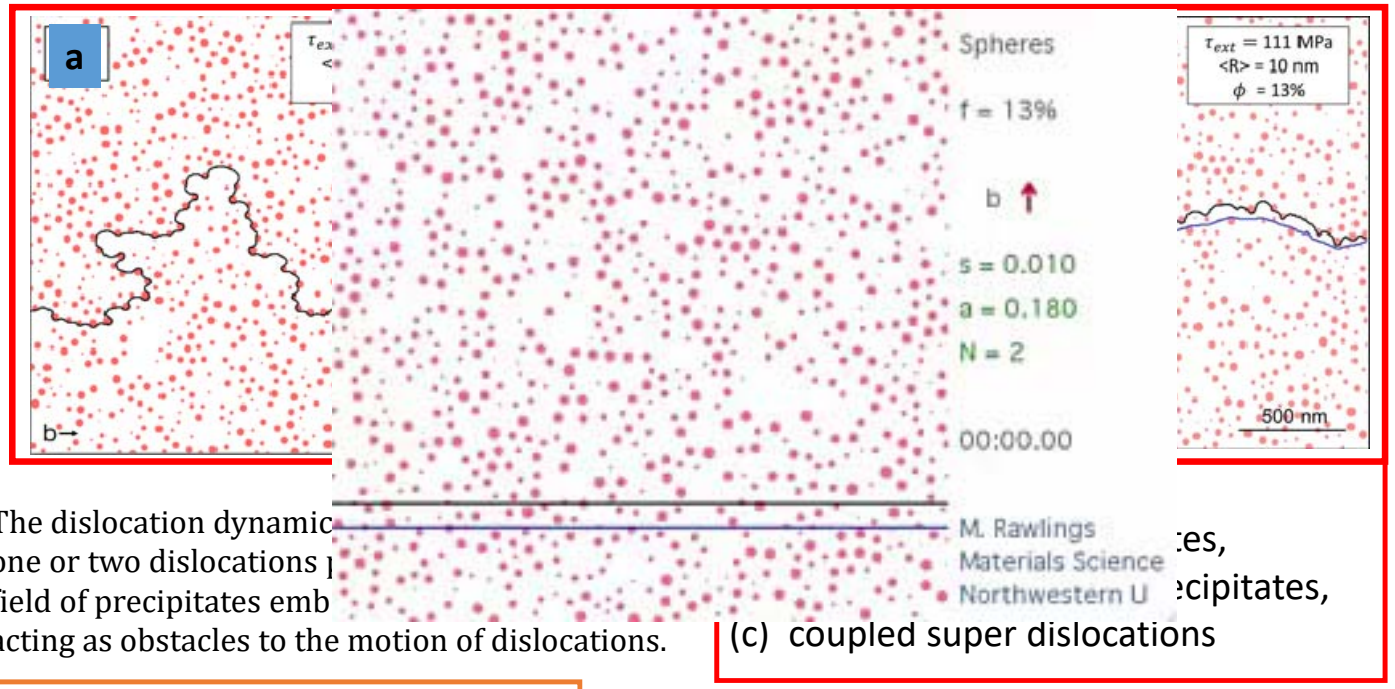

The dislocation dynamic
one or two dislocations
field of precipitates emb
acting as obstacles to the motion of dislocations.

es,
cipitates,

(c) coupled super dislocations

Line Dislocation Model

$$\tau_{ext} + \tau_{obst} + \tau_{dis} + \tau_{drag} = 0$$

where τ_{ext} is the external stress applied to the system, τ_{obst} is the stress associated with the dislocation interacting with the precipitates, τ_{disloc} is the stress induced by the dislocation interacting with itself and/or other dislocations and τ_{drag} is the stress due to viscous drag which is proportional to the nodes local velocity normal to the dislocation line

M. J. S. Rawlings, D. C. Dunand To be submitted, NU

Plot of estimated strengthening

Several equations predict the strengthening increment τ_p for alloys containing precipitate or dispersoids with volume fraction ϕ and radii <R>,

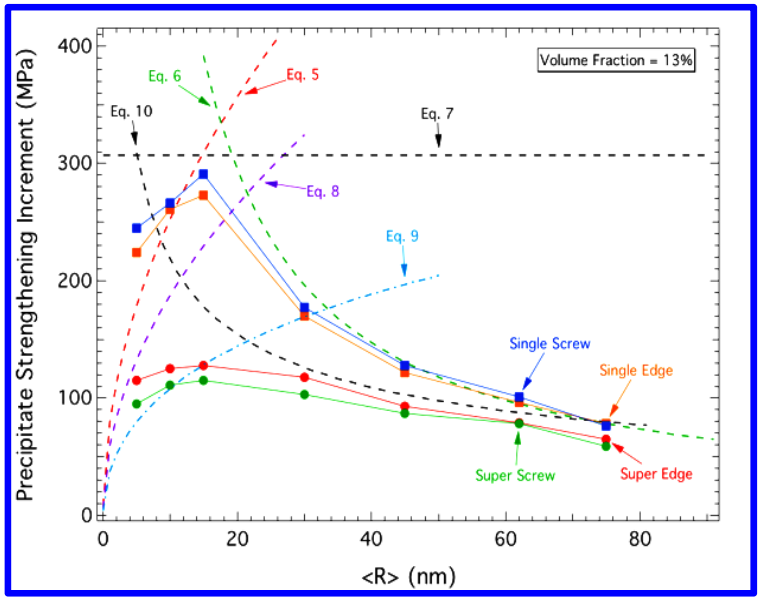

Plot of estimated strengthening increment, $\boldsymbol{\tau_p}$, in Fe alloys with β'(B2)-precipitates with an APB energy of 200 mJ m^{-2} as a function of precipitate average radius with volume fraction ϕ= 13% for DD-simulations

Main equations

Friedel equation for the case where the particles are sheared (eq 5)

$$\tau_p^{Friedel} = \frac{2S}{b\langle R\rangle\sqrt{\pi\omega_q}}\sqrt{\phi}\left(\frac{\gamma_{APB}\omega_r\langle R\rangle}{S}\right)^{3/2}$$

where ω_r and ω_q are spherical correction constants which take into account for 2-D planes cutting 3-D spherical particles and have values of $\omega_r = 0.82$ and $\omega_q = 0.75$, and where $S = \mu b^2/2$ denotes the line tension, with μ the shear modulus.

Orowan equation for describing a bypass the particles by the looping mechanism (eq 6)

$$\tau_p^{Orowan} = \frac{2S}{b\omega_L\langle R\rangle}$$

where ω_L is $\sqrt{\pi\omega_q/\phi} - 2\omega_r$,

M. J. S. Rawlings, D. C. Dunand To be submitted, NU

Other equations

In the case of a square lattice, the maximum force, F_0 , of a particle and the minimum inter-particle distance,λ_{E-E}^{min}, are employed to determine a theoretical peak strengthening

Eq. 7 $$\tau_p^{Square\ Lattice} = \frac{F_0}{b\lambda_{E-E}^{min}} = \frac{2\omega_r}{\sqrt{\pi\,\omega_q/\phi}}\frac{\gamma_{APB}}{b} \quad \text{with } F_0 = 2\gamma_{APB}\omega_r\langle R\rangle$$

For alloys in the under-aged condition where the shearing mechanism is dominant, the strengthening increment is:

Eq. 8 $$\tau_p^{underaged} = \frac{\gamma_{APB}}{2b}\left\{\left(\frac{4\omega_r^3}{\pi\omega_q}\right)^{\frac{1}{2}}\left[\frac{\gamma_{APB}\langle R\rangle\phi}{S}\right]^{\frac{1}{2}} - \alpha\phi\right\}$$

for alloys with high volume fractions of particles

Eq. 9 $$\tau_p^{HVf} = \frac{\gamma_{APB}}{2b}\{u - \alpha\phi\}$$, where $u = \frac{-B+\left(\frac{B^2}{3}+4B\right)^{1/2}}{2\left(1-\frac{B}{6}\right)}$ and $B = \frac{3\pi^2\gamma_{APB}\langle R\rangle\phi}{32S}$.

Finally, for shearing of particles by closely-coupled dislocation, where two dislocations reside in the same particle, the following equation was derived

Eq. 10 $$\tau_p^{SP} = 0.69\left(\frac{\gamma_{APB}p\phi S}{b^2\langle R\rangle}\right)^{\frac{1}{2}}$$, where p is a fitting parameter equal to unity.

Creep Behavior

Aging temperature effect on creep resistance

Materials: Fe-2Ti-6.5Al-10Cr-10Ni-3.4Mo-0.25Zr-0.005B (wt.%)

Homogenized at 1,200 °C for 0.5 h, then:

- **aged: 700, 740, 780 °C for 100 h**
- **creep test: at 700 °C under stress ranging from 70 – 270 Mpa**
- **added condition for comparison: aged 700 °C for 900 hr**

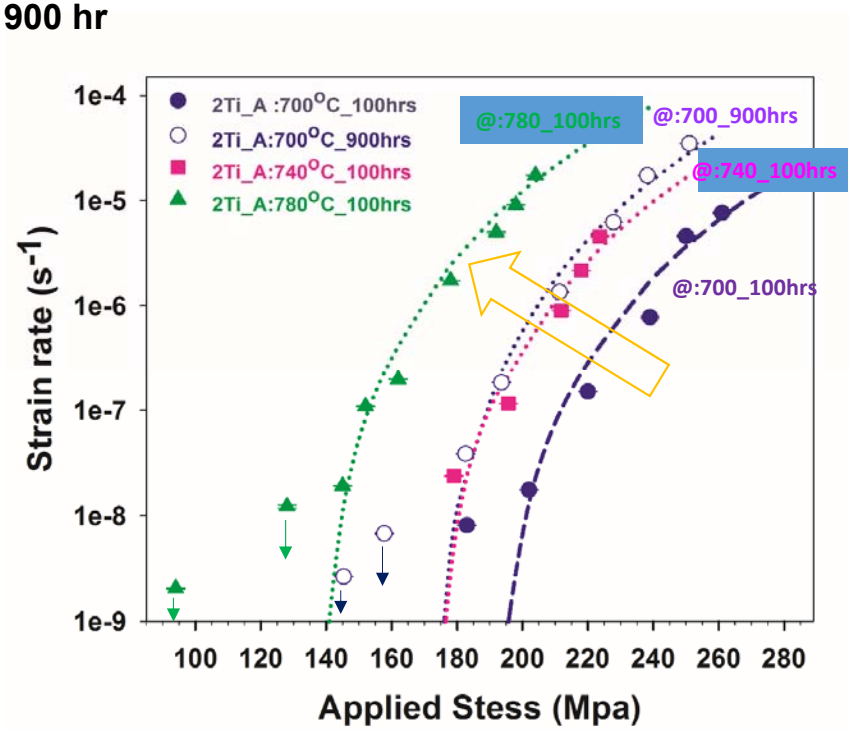

Creep strain rate vs applied stress

$$\dot{\varepsilon}_s = A\frac{\mu bD}{kT}\left(\frac{\sigma-\sigma_{th}}{\mu}\right)^n$$

where A is a constant, μ is the shear modulus, D is the effective diffusion coefficient, k is the Boltzmann constant, T is the temperature, σ_{th} is the threshold stress, and n is the creep-stress exponent

Threshold stress of the FBB8+2Ti ferritic alloy with different aging temperature

Sample tested	Threshold stress (Mpa)
Aged @ 700°C for 100hr Tested:700°C	179
Aged @ 740°C for 100hr	168.2
Aged @ 780°C for 100hr	135.5
Aged @ 700°C for 900hr	169.1

Manuscript in preparation, NU

Microstructure Comparisons

Chemical etching + SEM observations

Aged at 700°C for 100 hrs

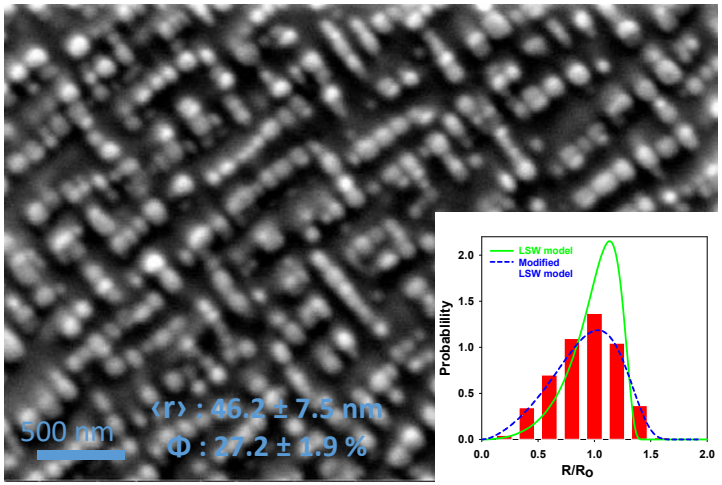

Aged at 780°C for 100 hrs

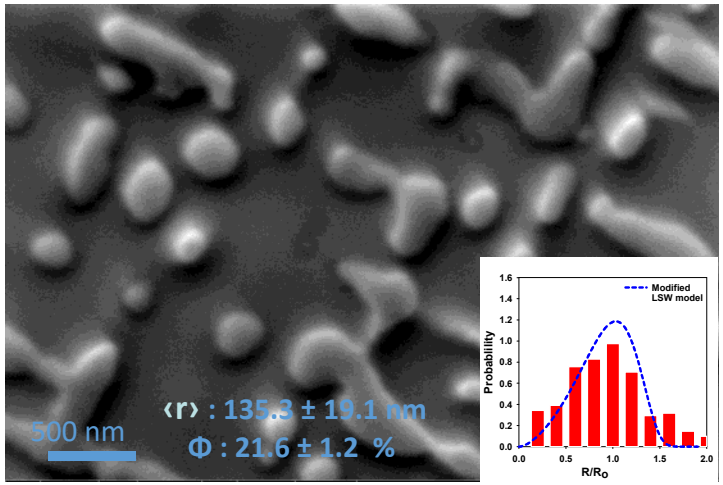

Aging temperature **increase** (from 700°C to 780°C for 100hr) → mean precipitate size ‹r› **increases** (from 46.2 ± 7.5 nm to 132.5 ± 19.1 nm) and area fraction (Φ) **decreases** (from 27.2 ± 1.9 to 21.6 ± 1.2 %) at the 2wt.%Ti +FBB8 sample

This is relating with the threshold stress change of 2wt.% Ti +FBB8 sample (decreases from 179± 1 MPa at 700°C to 135.5 ± 2 Mpa at 780°C for 100hrs aging time).

Creep Behavior II (cont'd)

Aging temperature + Creep temperature effect

Aged 760 and 800 °C, Creep test temperature at 700 and 740 °C

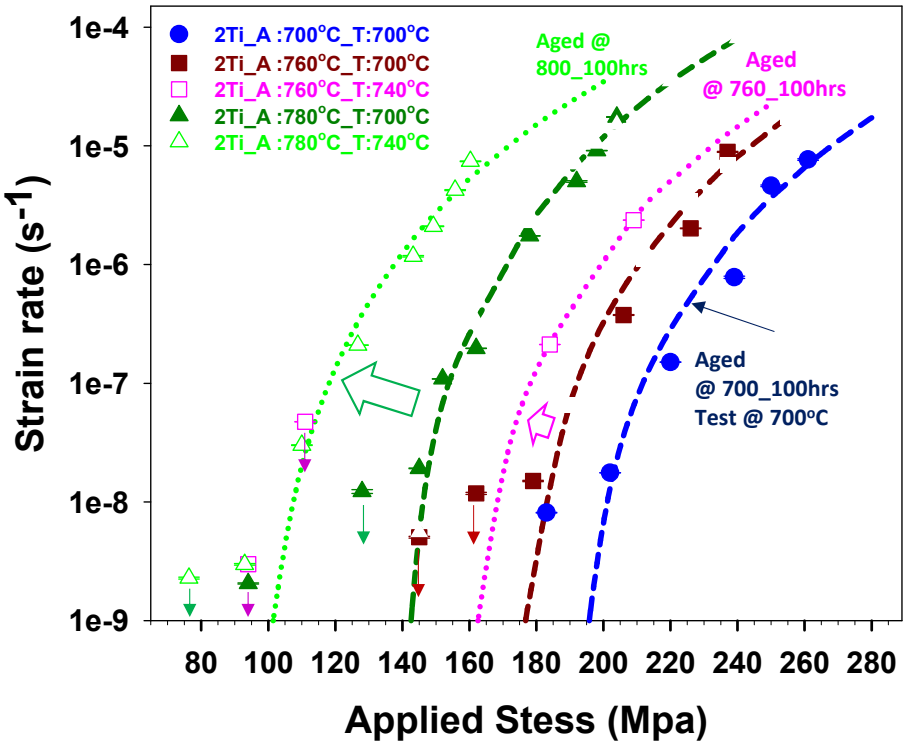

Threshold stress of the FBB8+2Ti ferritic alloy with different operating creep temperature	
Sample tested	**Threshold stress (MPa)**
Aged @ 700°C for 100hr, Tested:700°C	179
Aged @ 760°C for 100hr Tested:700°C	167.9
Aged @ 760°C for 100hr Tested:740°C	154.1
Aged @ 800°C for 100hr Tested:700°C	129.8
Aged @ 800°C for 100hr Tested:740°C	71.2

13.8 MPa decrease

57.8 MPa decrease

Manuscript in preparation, NU

Microstructure Comparisons

SEM observations

Aged at 760°C for 100 hrs

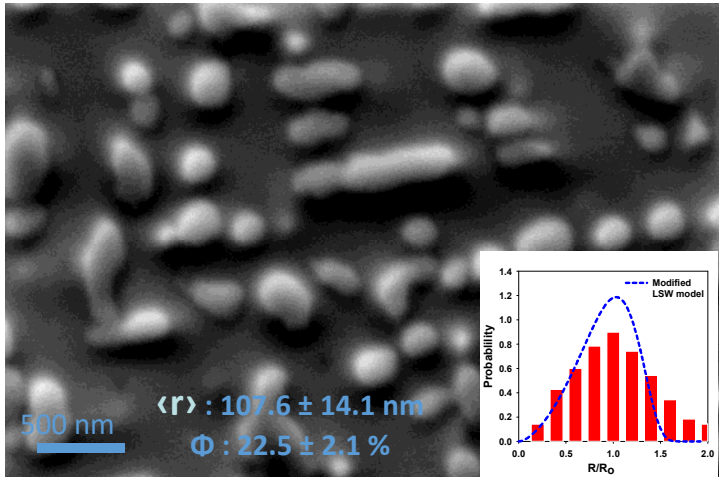

Aged at 800°C for 100 hrs

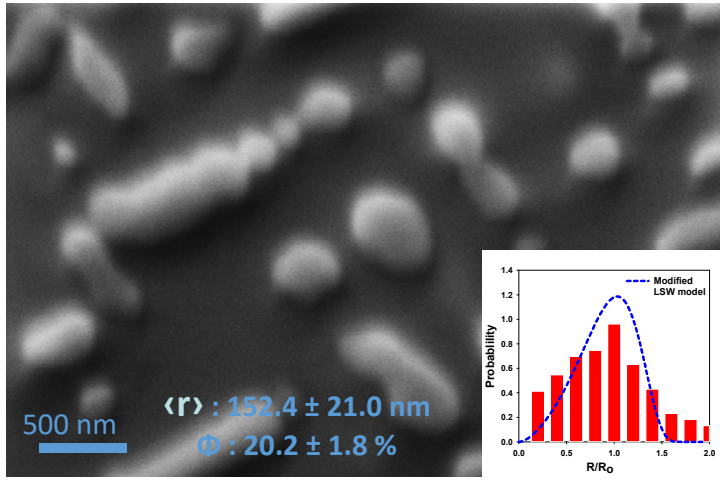

Aging temperature **increase** (from 760°C to 800°C for 100hr) → mean precipitate size ‹r› **increases** (from 107.6 ± 14.1 nm to 152.4 ± 21.0 nm) and area fraction (Φ) **increases** to from 22.5 ± 2.1 to 20.2 ± 1.8 % at the 2wt.%Ti +FBB8 sample

The larger size and smaller fraction of precipitate decrease the Orowan stress between precipitate and matrix, that might be introduce the decrease the larger threshold stress in the 2wt.% Ti +FBB8 sample aged at 800 °C for 100hrs than 760 for 100hr. (the amount of decreases increase to 57.8 ± 4 MPa at the 800°C aged sample from 13.8 ± 4 MPa at 780°C sample). The other possibility is the increase of austenite transformation at the higher temperature.

Aging time effect for 2wt% Ti+FBB8

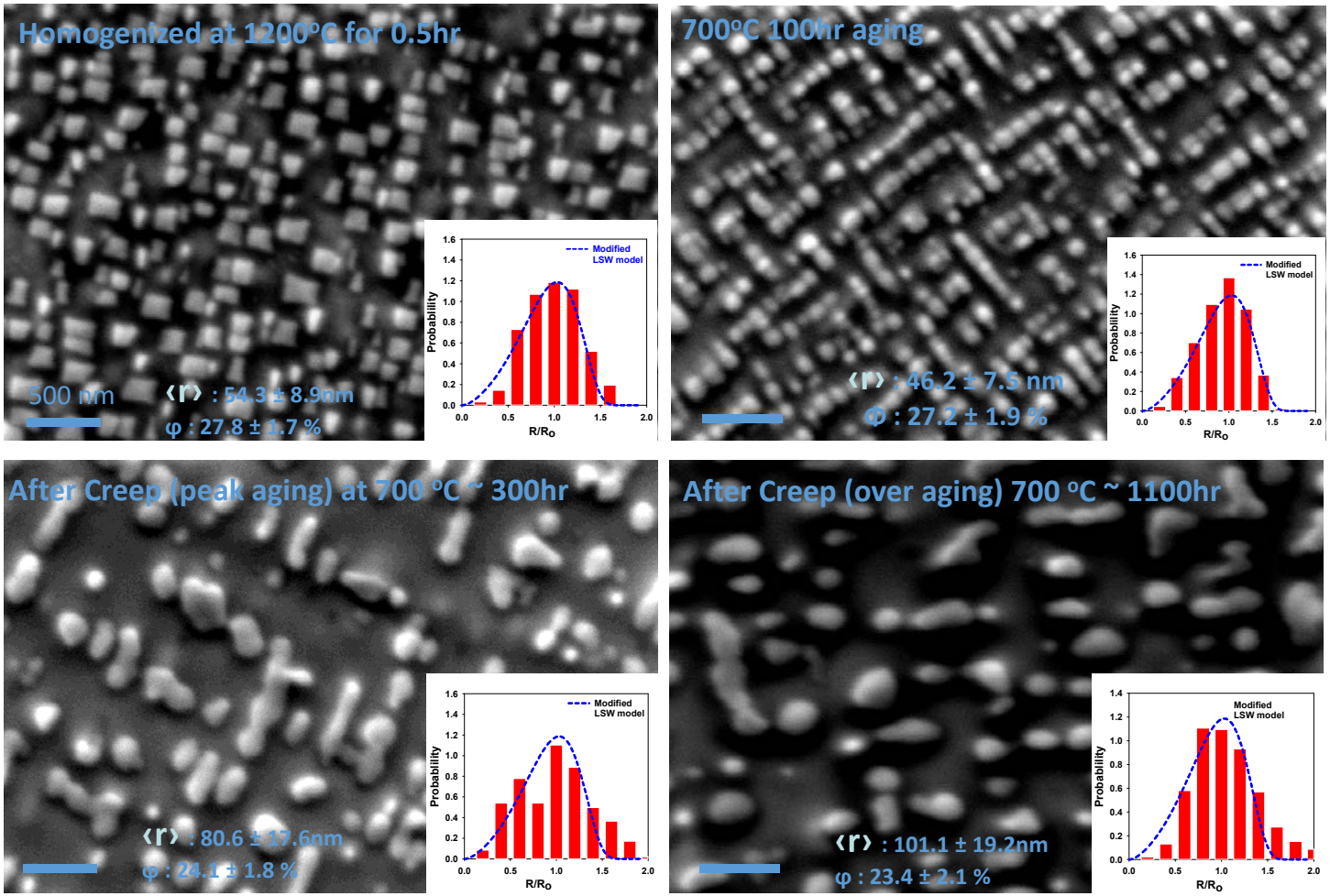

Precipitate growth by interconnection of precipitates. Volume fraction is decreased during annealing.
Matrix's orientation effect is not included

Radius and fraction changes with aging time (2wt.% Ti sample)

Coherency breaking after 500 hrs aging

BF-TEM (G. Song et al. / Acta Materialia 127 (2017))

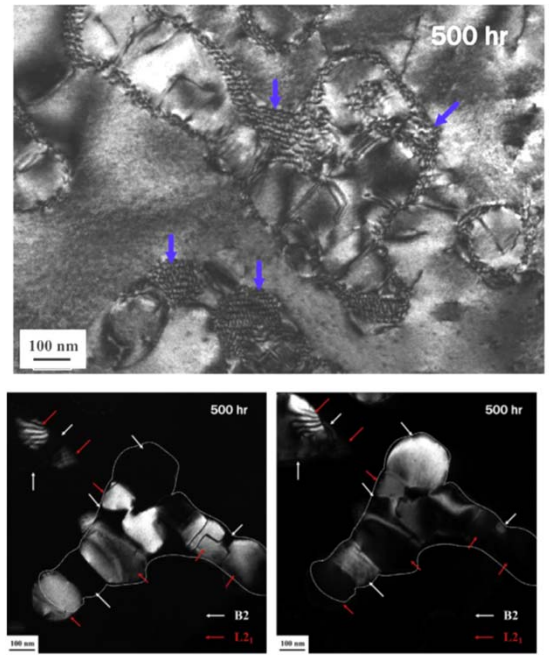

Segregation of $L2_1$ structure + radius increase during aging

Radius change with aging time at 700oC in 2wt.% Ti alloy

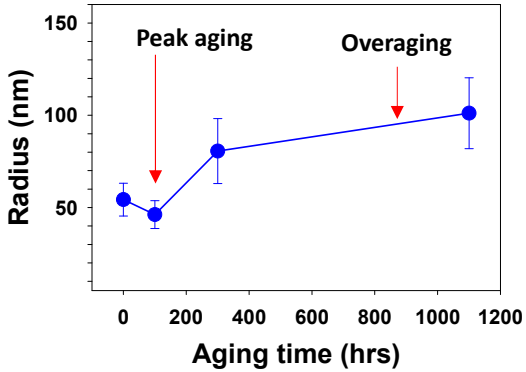

Fraction change with aging time at 700oC in 2wt.% Ti alloy

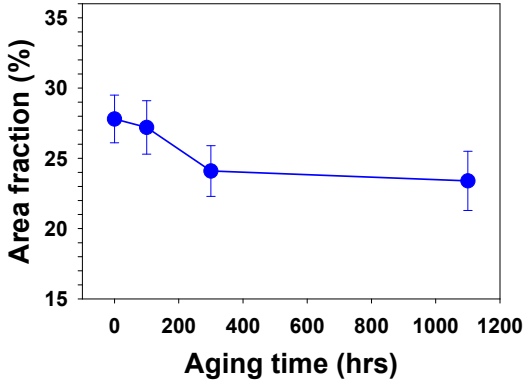

Creep Behavior III (cont'd)

Hf addition effect

Materials: Fe - 0.5Hf - 1.5Ti - 6.5Al-10Cr-10Ni-3.4Mo-0.25Zr-0.005B (wt.%)

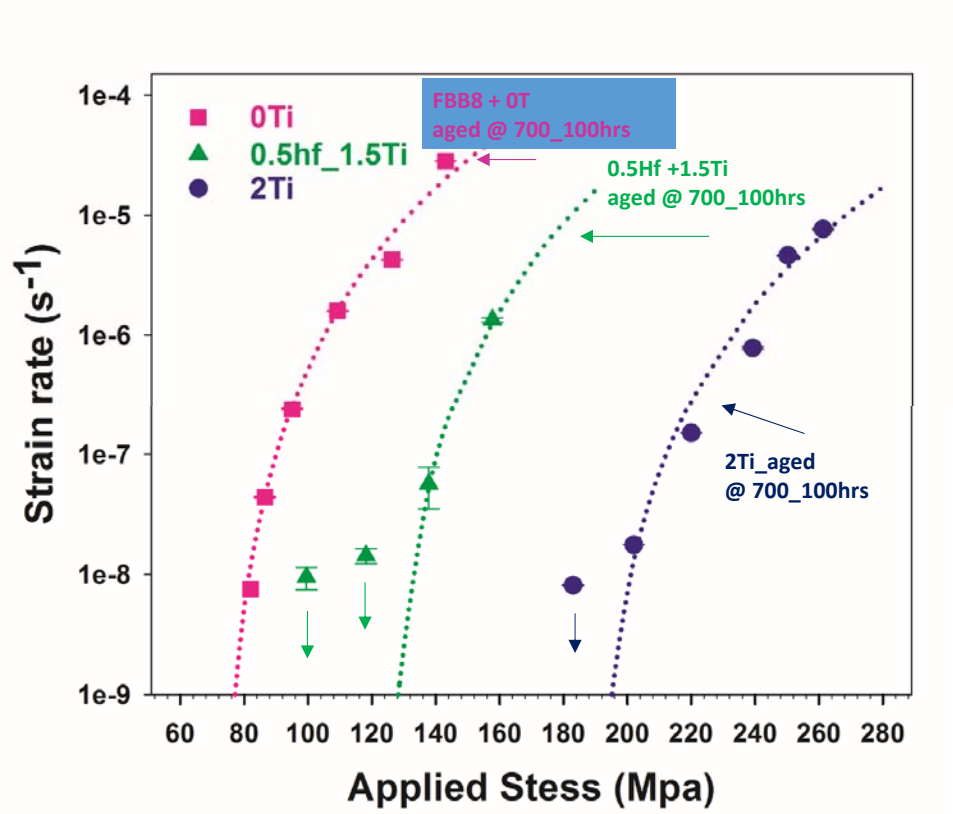

Threshold stress of the FBB8, 0.5Hf+0.5Ti, 2Ti ferritic alloy Aged @ 700°C for 100hrs Tested @ 700°C	
Sample tested	**Threshold stress (MPa)**
FBB8 (0%Ti) Aged @ 700 for 100hrs Tested at 700°C	70.8
FBB8+0.5%Hf+1.5%Ti	121.5
Aged @ 780 for 100hrs	179

Manuscript in preparation, NU

Microstructure Comparisons

SEM observations

Aged at 700°C for 100 hrs

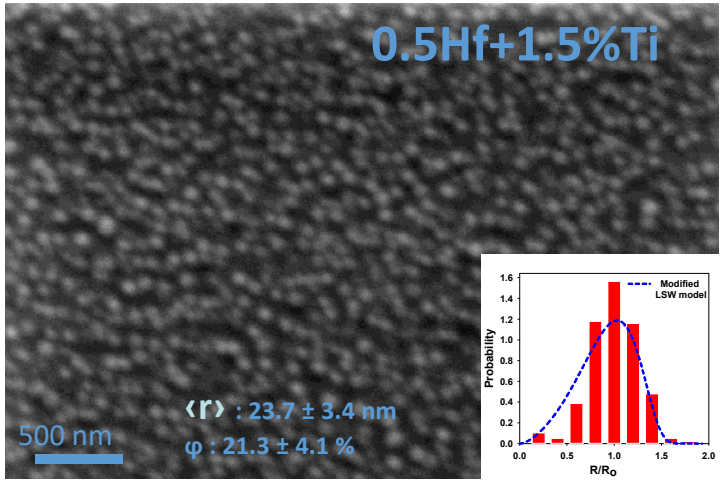

Crept sample ~ 300 hrs aging @700 °C

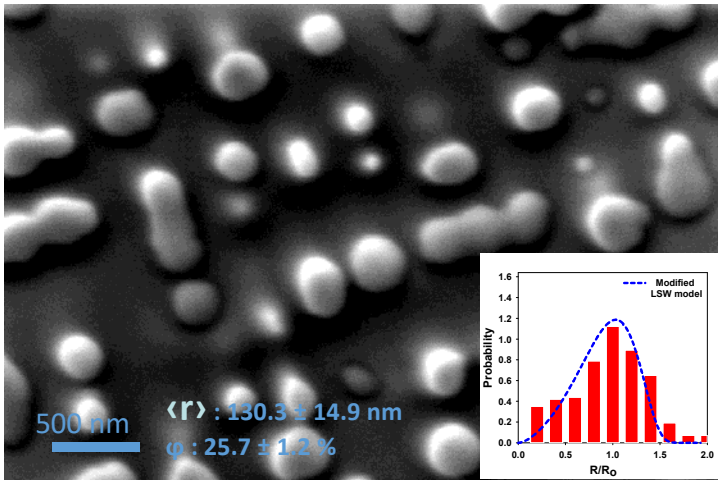

The addition of (0.5wt%Hf+ 1.5wt%Ti) in FBB8 sample → mean precipitate size **decreases** (to 23.7 ± 3.4 from 46.2 ± 7.5 nm at 2wt.% Ti sample aging 700 °C for 100hr) and area fraction **decreases** (to 21.3 ± 4.1 from 27.2 ± 1.9 % at 2wt. % Ti sample aging 700 °C for 100hr). But the growth rate of the precipitate during creep (~300hrs) in the 0.5Hf+1.5Ti sample is much faster than 2wt.% Ti sample (mean radius = 130.3± 14.9 nm, area fraction=25.7± 1.2) which is relating with decrease of creep resistance with respect to the 2wt.% Ti+FBB8 sample.

Atom Probe Tomography Study at northwestern Univ.

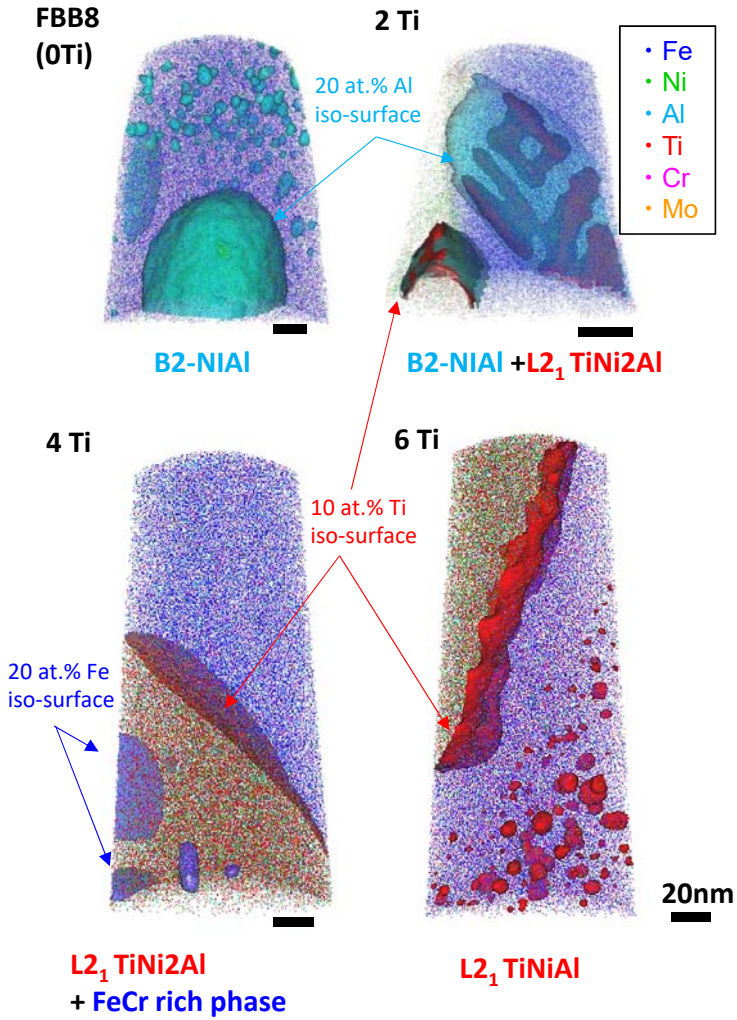

Time of flight Mass spectrum analysis

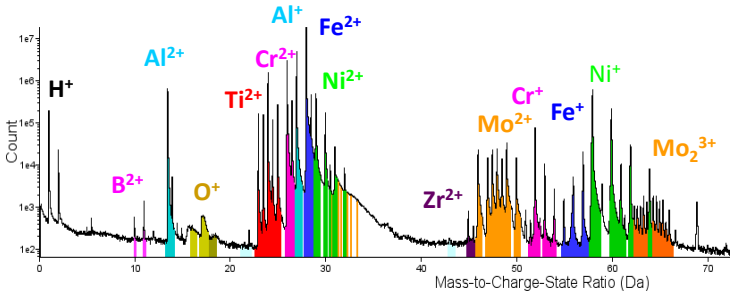

Average concentrations in precipitates

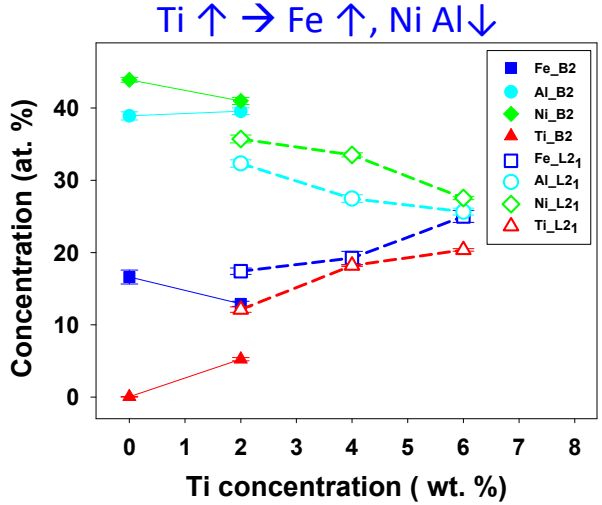

S.I. Baik, D. Dunand, Unpublished, NU

Atom Probe Tomography (cont'd)

2Ti

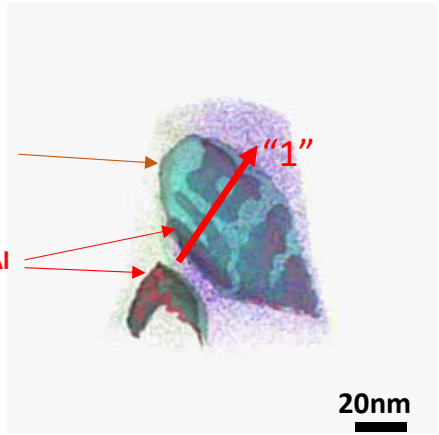

Concentration along the arrow "1"

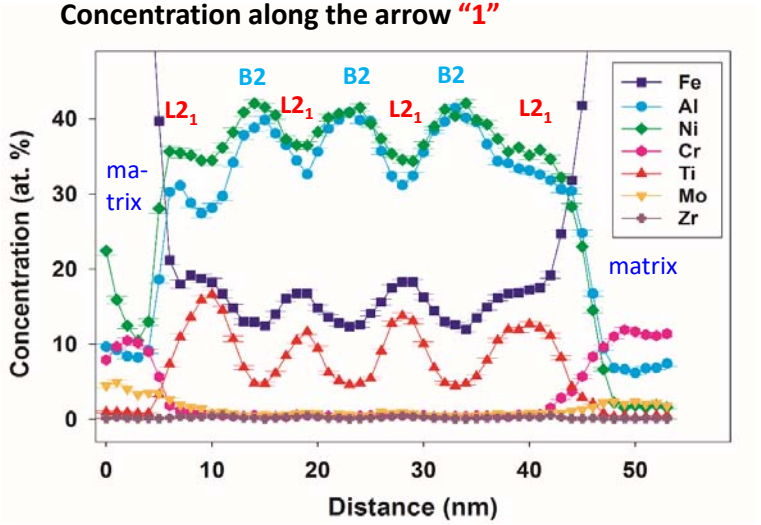

4Ti

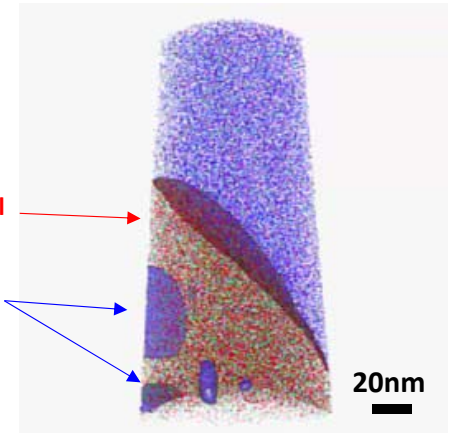

Two proximity concentration histograms across BCC matrix - L2$_1$ - FeCr rich precipitates

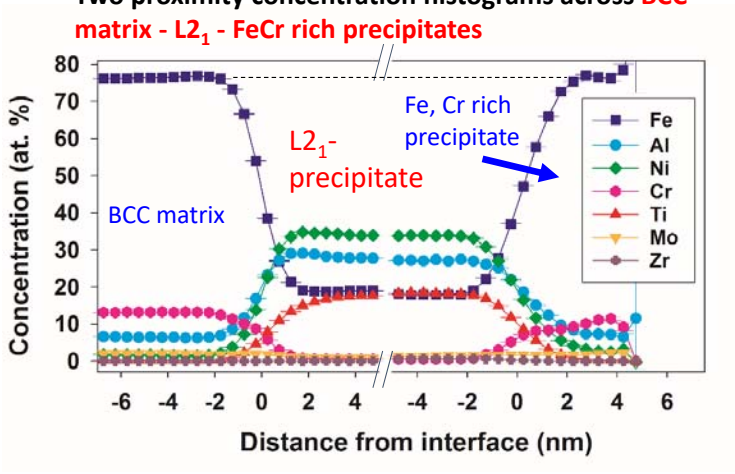

Size difference with Ti concentration

(after homogenization at 1200°C for 0.5hr)

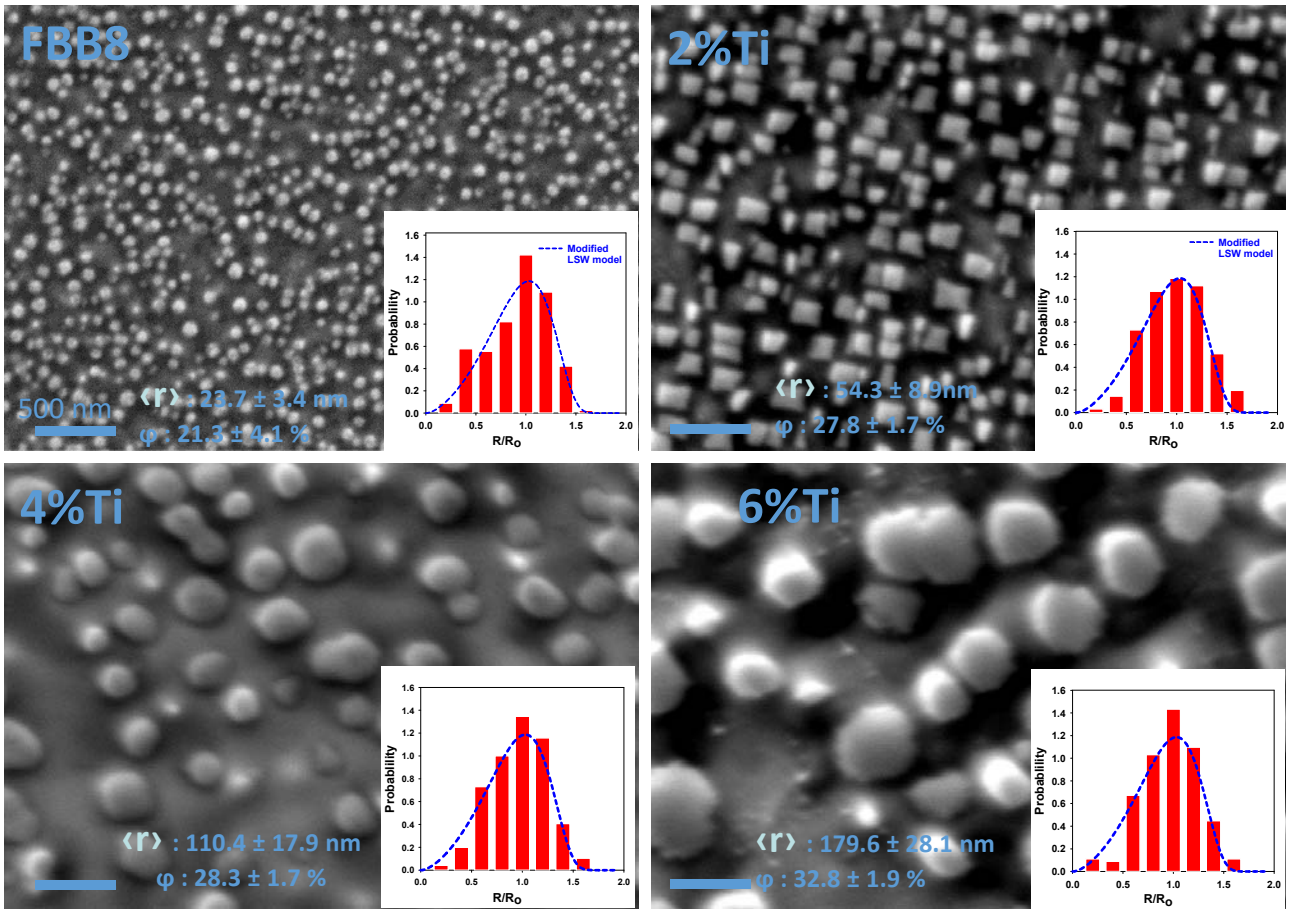

Radius and fraction changes with Ti additions

Creep behavior in 0-6 wt.Ti +FBB8 Ferritic alloy,

Threshold values in Creep experiment

Test:100 at 700°C

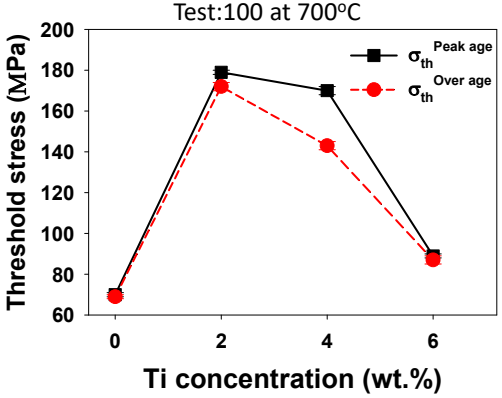

Michael J.S. Rawlings et al.// Acta Materialia 128 (2017)

BF-TEM image for 4wt% Ti samole after homogenization-treated at 1473 K for 0.5 h

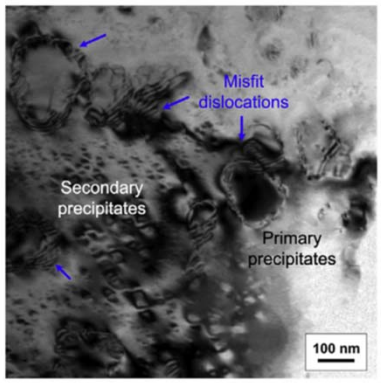

G. Song et al. / Acta Materialia 127 (2017)

Radius change with 0-6 wt%Ti concentration after homogenization

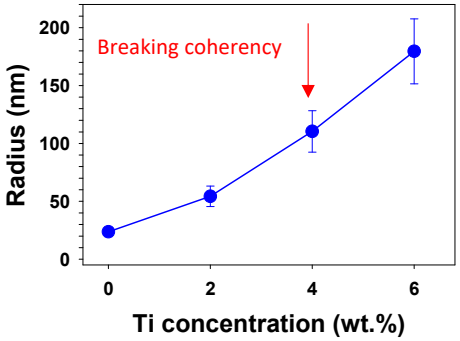

Area fraction change with 0-6 wt%Ti.

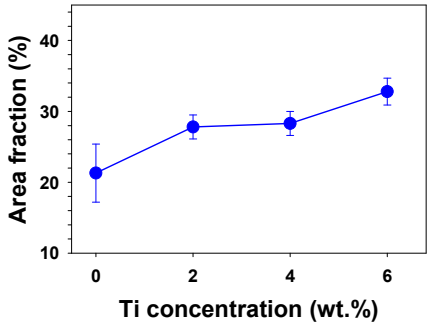

Precipitate size and volume fraction increase with Ti addition. The coherency is breaking at 4% which might be from the $L2_1$ structure + radius? increase → $L2_1$ volume fraction and also size control are needed.

Summary

- The effect of aging temperature and creep operating temperature was investigated in the relationship with creep resistance of 2wt.% Ti +FBB8 samples.
- The addition of Hf (0.5wt%) in the 1.5wtTi+FBB8 sample increase of creep resistance with respect to FBB8 sample, but not to the 2wt.% Ti+FBB8 sample.
- The concentration and morphology changes was observed with the Ti concentration increase. As Ti concentration increase, Fe concentration is also increase in the precipitate, but Ni and Al concentration decreases. Only 2wt.% Ti shows the cuboidal shape of precipitate.

Further works

Final adjustment for a maximum values of creep properties

1. Ti concentrations at 2.5, 3, 1.5 wt.%.
2. Controlling the precipitate size, volume fraction by additional heat treatment and/or elements.
3. Develop the model for creep mechanisms

3wt% Ti after 100hrs aging at 700°C

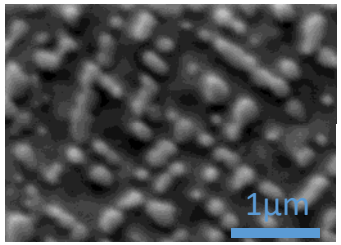

Current Progress - Comparison between Zr and Hf

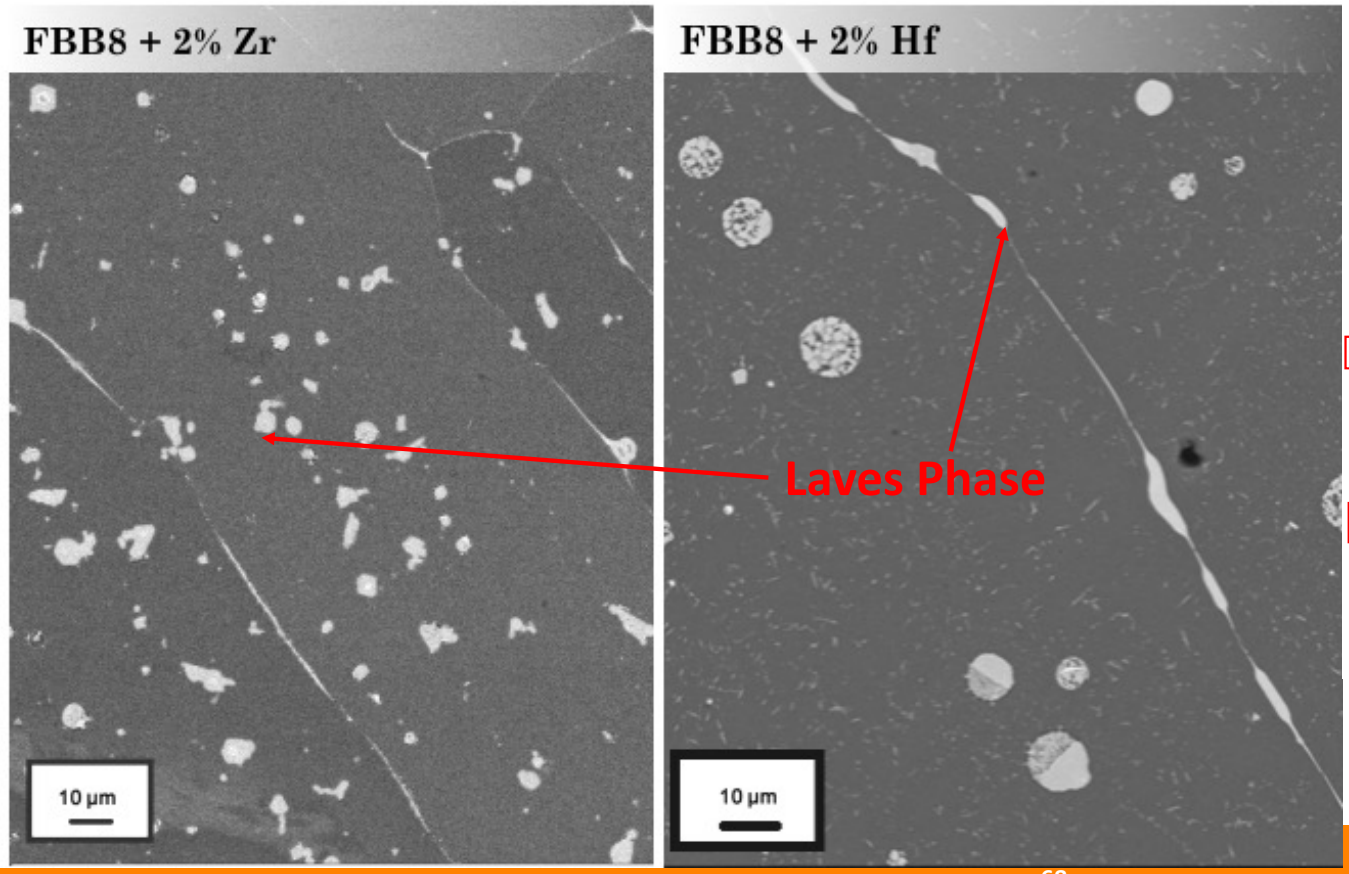

Phase	Space Group
α-Zr	$P6_3/mmc$
β-Zr	$Im\bar{3}m$
α-$ZrCr_2$ *C15*	$Fd\bar{3}m$
β-$ZrCr_2$ *C36*	$P6_3/mmc$
γ-$ZrCr_2$ *C14*	$P6_3/mmc$
$ZrFe_2$ *C15*	$Fd\bar{3}m$
$ZrFe_2$ *C36*	$P6_3/mmc$
$ZrFe_2$ *C14*	$P6_3/mmc$
Zr_2Fe	$I4/mcm$
Zr_2Ni	$I4/mcm$

	Experiments
Fe	Fe_2Hf(C14, C15)
	$FeHf_2(NiTi_2)$

P. A. Burr, S. T. Murphy, S. C. Lumley, M. R. Wenman, and R. W. Grimes, Corrosion Science, Vol. 69 (2013) 1–4
O. Levy, G. L. W. Hart, and S. Curtarolo, Acta Mater., Vol. 58, 8 (2010) 2887-2897.

Current Progress - CALPHAD Calculations (Cont'd)

- Phase diagram for the FBB8 + Hf system cannot be obtained in this method due to lack of database.

- The FBB8 + Ti system shows the presence of $L2_1$ phase.

- However, in the FBB8 + Zr system, there's no $L2_1$ phase formed. Instead, Laves phase formed in the FBB8 + Zr system.

Current Progress - Creep Tests (Cont'd)

Aging Temperature & Time Effect

Homogenized at 1,200 °C for 0.5 h, then:

- **aged: 700, 740, 780°C for 100 h**
- **creep test under stress ranging from 70 – 270 MPa**
- **added for comparison: aged 700 °C for 900 h**

Creep strain rate vs applied stress

$$\dot{\varepsilon}_s = A\frac{\mu b D}{kT}\left(\frac{\sigma-\sigma_{th}}{\mu}\right)^n$$

where A is a constant, μ is the shear modulus, D is the effective diffusion coefficient, k is the Boltzmann constant, T is the temperature, σ_{th} is the threshold stress, and n is the creep-stress exponent

Threshold stress of the FBB8+2Ti ferritic alloy with different aging temperature	
Sample tested	Threshold stress (MPa)
Aged @ 700 °C for 100 h	179
Aged @ 740 °C for 100 h	166.2
Aged @ 780 °C for 100 h	135.5
Aged @ 700 °C for 900 h	169.1

* In preparation, NU

Current Progress - Creep Tests (Cont'd)

Aging Temperature & Time Effect

Materials

•Fe-2Ti-6.5Al-10Cr-10Ni-3.4Mo-0.25Zr-0.005B (wt.%)

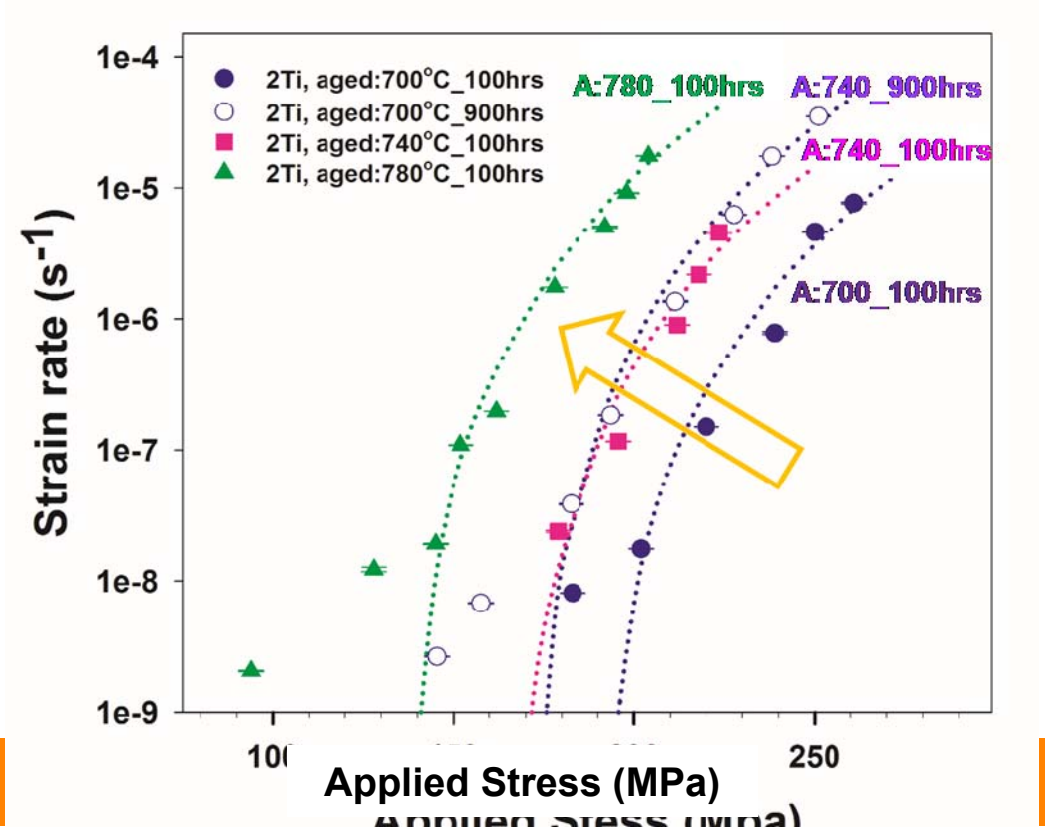

* In preparation, NU

Current Progress - Creep Tests (Cont'd)

Aging Temperature & Time Effect

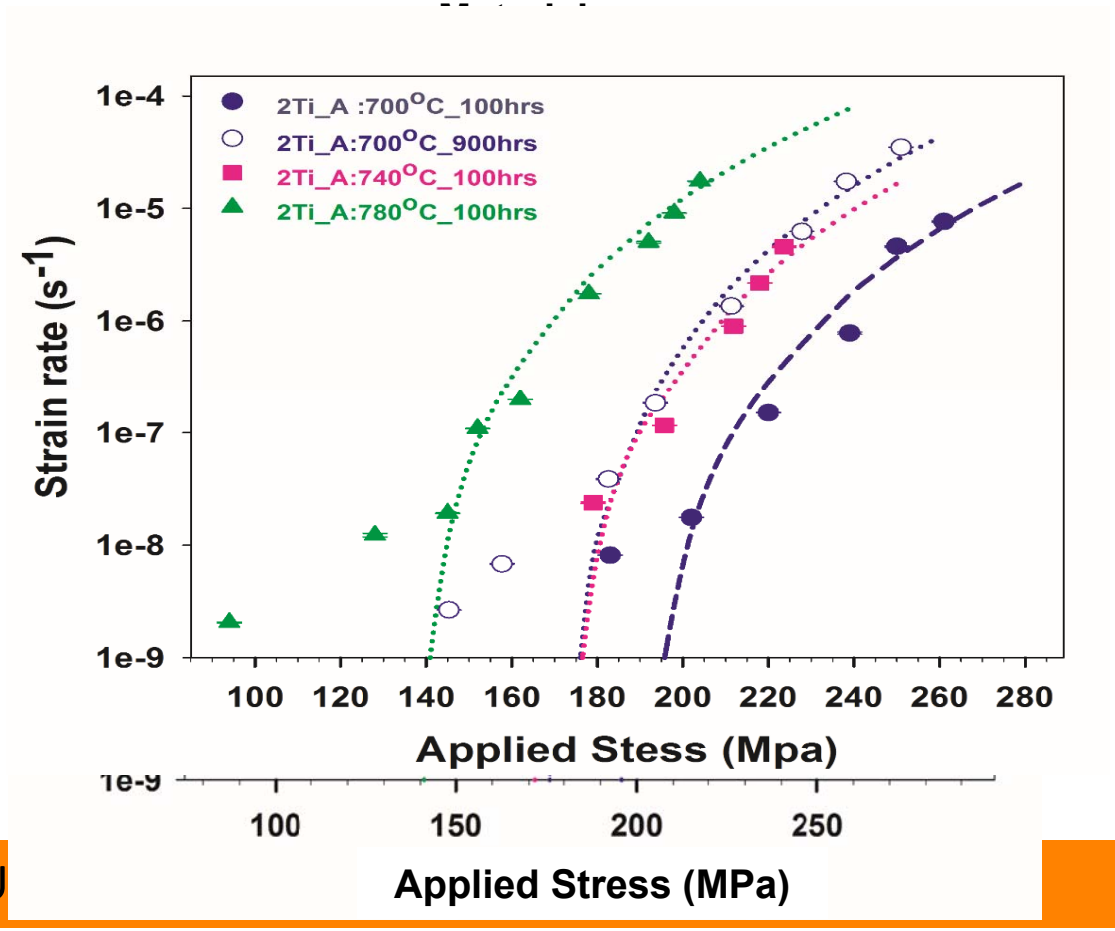

* In preparation, NU

Current Progress - Creep Tests (Cont'd)

Aging Temperature & Time Effect

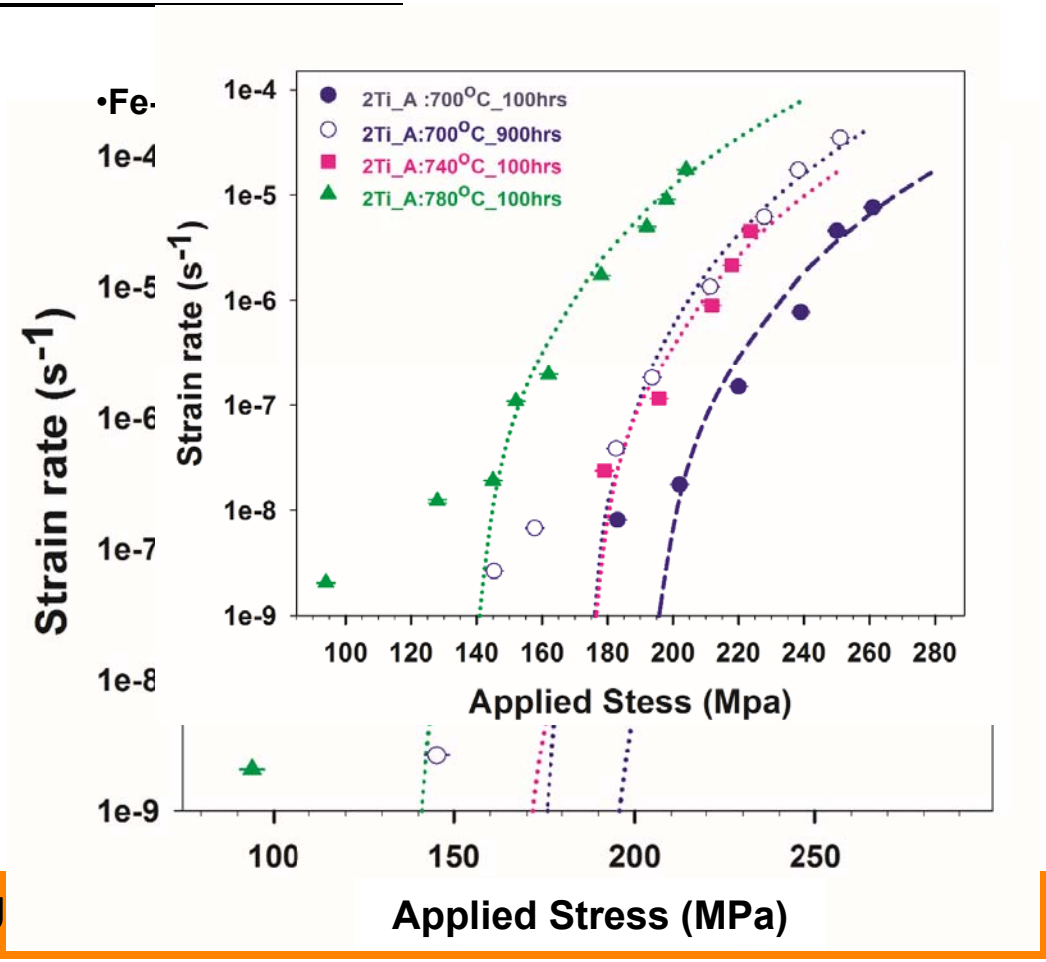

* In preparation, NU